

INFORMATION TO USERS

This manuscript has been reproduced from the microfilm master. UMI films the text directly from the original or copy submitted. Thus, some thesis and dissertation copies are in typewriter face, while others may be from any type of computer printer.

The quality of this reproduction is dependent upon the quality of the copy submitted. Broken or indistinct print, colored or poor quality illustrations and photographs, print bleedthrough, substandard margins, and improper alignment can adversely affect reproduction.

In the unlikely event that the author did not send UMI a complete manuscript and there are missing pages, these will be noted. Also, if unauthorized copyright material had to be removed, a note will indicate the deletion.

Oversize materials (e.g., maps, drawings, charts) are reproduced by sectioning the original, beginning at the upper left-hand corner and continuing from left to right in equal sections with small overlaps. Each original is also photographed in one exposure and is included in reduced form at the back of the book.

Photographs included in the original manuscript have been reproduced xerographically in this copy. Higher quality 6" x 9" black and white photographic prints are available for any photographs or illustrations appearing in this copy for an additional charge. Contact UMI directly to order.

UMI

A Bell & Howell Information Company
300 North Zeeb Road, Ann Arbor, MI 48106-1346 USA
313/761-4700 800/521-0600

A

Performance Degradation of Multiwavelength Optical Networks due to Laser and Optical (De)multiplexer Misalignments

by

Nidal Nuri Khrais

A dissertation submitted to the Graduate Faculty in Engineering in
partial fulfillment of the requirement for the degree of Doctor of
Philosophy, The City University of New York

1996

UMI Number: 9707114

**Copyright 1996 by
Khrais, Nidal Nuri**

All rights reserved.

**UMI Microform 9707114
Copyright 1996, by UMI Company. All rights reserved.**

**This microform edition is protected against unauthorized
copying under Title 17, United States Code.**

UMI
300 North Zeeb Road
Ann Arbor, MI 48103

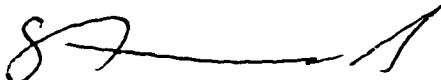
© 1996

NIDAL NURI KHRAIS

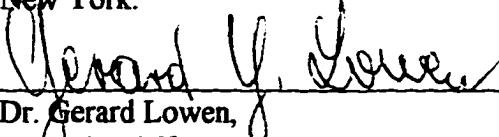
All Rights Reserved

This manuscript has been read and accepted by the Graduate Faculty in Engineering in satisfaction of the dissertation requirement for the degree of Doctor of Philosophy.

9/3/96
Date


Prof. Samir Ahmed,
Chair of Examining Committee, Mentor,
Department of Electrical Engineering, The
City College of the City University of
New York.

9/12/96
Date


Dr. Gerard Lowen,
Executive Officer,
Associate Dean for Graduate Studies
in Engineering, The City College of the City
University of New York.

Other members of examining committee:

Prof. Fred Moshary, Associate Professor, Department of Electrical Engineering,
The City College of the City University of New York.

Prof. Mohamed Ali, Associate Professor, Department of Electrical Engineering,
The City College of the City University of New York.

Prof. Leonid Roytman, Professor, Department of Electrical Engineering, The City
College of the City University of New York.

Prof. Tarek Saadawi, Professor, Department of Electrical Engineering, The City
College of the City University of New York.

Dr. Aly Elrefaie, Senior Scientist, Co-mentor, Hewlett Packard,
Palo Alto, California.

Dr. Demetri Kokkinos, Nynex, White Plains, New York.

THE CITY UNIVERSITY OF NEW YORK

Abstract

Performance Degradation of Multiwavelength Optical Networks due to Laser and Optical (De)multiplexer Misalignments

by

Nidal Nuri Khrais

Advisor: Professor Samir Ahmed

Laser misalignment tolerances for Wavelength Division Multiplexing (WDM) systems with two optical (de)multiplexers are almost the same at 2.5 Gb/s and 10 Gb/s per optical channel. For the three types of (de)multiplexers considered, (de)multiplexers modeled as third-order Butterworth filters have the highest misalignment tolerances, (de)multiplexers modeled as second-order Butterworth filters have lower misalignment tolerances, and (de)multiplexers modeled as first-order filters have the lowest misalignment tolerances. Using two (de)multiplexers

modeled as second-order Butterworth filters, laser misalignments of about ± 30 GHz for 25 GHz (de)multiplexer misalignments produce 1 dB system excess loss. Even though the 1 dB system excess loss is a distortion-free criteria, it is found to produce very stringent misalignment tolerances. A more practical criteria occurs at 0.3 dB distortion-induced eye-closure penalty where the eye-diagram still looks good. Laser misalignment tolerances for WDM optical networks with a cascade of 2 to 100 (de)multiplexers modeled as either first-order filters or third-order Butterworth filters are evaluated at 0.3 dB distortion-induced eye-closure penalty. The results are dependent on the number of (de)multiplexers used, on the bit rate, and on the filter characteristic. We find that both the magnitude and the phase characteristics of the (de)multiplexers transfer function are important in determining the distortion-induced penalties. The allowable laser misalignment tolerances, at 10 GB/s and for systems using (de)multiplexes modeled as third-order Butterworth filters, vary from ± 78 GHz (± 0.63 nm) for systems with a cascade of 2 filters to ± 18 GHz (± 0.15 nm) for systems with a cascade of 100 filters.

A (de)multiplexer model is formulated. This model is general for any bit rate, any filter shape and phase, with any bandwidth, and for any number of (de)multiplexers in cascade.

**In memory of my father Nuri Khrais,
to my mother Rashideh Khrais,
and to my wife Laila.**

Acknowledgments

I wish to express my gratitude to my thesis advisor Prof. S. Ahmed for his support and guidance throughout this work.

I also would like to express my appreciation to Dr. Aly Elrefaie. His support, guidance and encouragement were essential in making this work possible. His enthusiasm and friendship made this an enjoyable and rewarding experience. I am forever indebted to him.

Special thanks and appreciation to Dr. Richard Wagner of Bellcore. His support, guidance, persistence and encouragement gave me the motivation to achieve more.

I also would like to thank Bellcore for accommodating me as visiting doctoral student in their Optical Networking Research Department in Red Bank in New Jersey.

Finally, I thank the everlasting GOD who made all things possible, and through whom all things exist.

Contents

Chapter 1	Introduction.....	1
1.1	Multiwavelength Optical Networks: Definitions and Motivations.....	1
1.2	Optical Transmitter.....	4
1.3	Optical Multiplexers and Demultiplexers.....	5
Chapter 2	Performance Degradation of WDM Systems due to Laser and Optical Filter Misalignments at 1 dB System Excess Loss Criteria.....	8
2.1	Introduction.....	8
2.2	The System Model.....	9
2.3	Simulation Results for a cascade of a Multiplexer and a Demultiplexer.....	12
2.4	Conclusions for a Cascade of a Multiplexer and a Demultiplexer.....	14
2.5	Simulation Results for a Cascade of Large Number of Multiplexers and Demultiplexers.....	14
2.6	Conclusions for a Cascade of Large Number of Multiplexers and Demultiplexers.....	17

Chapter 3	Performance Degradation of Multiwavelength Optical Networks due to Laser and (De)multiplexer Misalignments for 30 (de)multiplexers in cascade.....	32
3.1	Introduction.....	32
3.2	The System Model.....	33
3.3	Simulation Results.....	38
3.4	Conclusion.....	40
Chapter 4	Performance of Cascaded Misaligned Optical (De)multiplexers in Multiwavelength Optical Networks for 2-100 (de)multiplexers in cascade.....	53
4.1	Introduction.....	53
4.2	The System Model.....	54
4.3	Simulation Results.....	56
4.4	Conclusions.....	58
Chapter 5	Multiplexer Eye-Closure Penalties for 10 Gb/s Signals in WDM Networks: Simulation Versus Experiment.....	67
5.1	Introduction.....	67
5.2	(De)multiplexer Model.....	68
5.3	Simulation and Experimental Results.....	69
5.4	Summary.....	70
Chapter 6	General (De)multiplexer Cascade Model for Transparent Digital Transmission.....	75

6.1	Introduction.....	75
6.2	(De)Multiplexer Model.....	76
6.3	System Model.....	79
6.4	Simulation Results.....	80
6.5	Example.....	81
6.6	Summary.....	82
	References.....	87

List of Tables

Table 2.1 Semiconductor laser parameter values used in solution of single-mode rate equations.....	29
Table 2.2 Laser frequency misalignment tolerances for a point-to point WDM systems with different types of optical filters.....	30
Table 2.3 Laser frequency misalignment tolerances for WDM systems using large number and different types of optical filters.....	31
Table 3.1 Misaligned (de)multiplexers distribution over a range of up to ± 12.5 GHz (± 0.1 nm).....	51
Table 3.2 Laser misalignment tolerances for WDM systems at 2.5 Gb/s or 10 Gb/s per optical channel with 30 (de)multiplexers modeled as either third-order or first-order Butterworth filters.....	52
Table 5.1 Optical multiplexer and demultiplexer characteristics.....	74
Table 6.1 Magnitude coefficients for 30 filters with $\theta(f)=0$	86

List of Figures

Figure 1.1	Progress in lightwave communication technology over the period 1974-1992. Different curves show the increase in the bit rate-distance product for five generations of fiber-optic communication systems.....	7
Figure 2.1	A Block diagram of typical WDM network architecture (system used in simulation is emphasized).....	18
Figure 2.2	Simulation block diagram for WDM system with a cascade of large number of multiplexers and demultiplexers.....	19
Figure 2.3	Laser spectrum and multiplexer/demultiplexer transmission characteristics.....	20
Figure 2.4	System excess loss at 2.5 Gb/s using direct current modulation of MQW-DFB laser.....	21
Figure 2.5	System excess loss at 2.5 Gb/s using direct current modulation of Bulk-DFB laser.....	22

Figure 2.6	System excess loss at 10 Gb/s using direct current modulation of MQW-DFB laser.....	23
Figure 2.7	System excess loss at 10 Gb/s using external modulation of a DFB laser.....	24
Figure 2.8	Laser spectrum under modulation at 2.5 Gb/s using direct current modulation of a Bulk-DFB laser.....	25
Figure 2.9	Laser spectrum under modulation at 2.5 Gb/s using direct current modulation of a MQW-DFB laser.....	26
Figure 2.10	Laser spectrum under modulation at 10 Gb/s using direct current modulation of a MQW-DFB laser.....	27
Figure 2.11	Laser spectrum under modulation at 10 Gb/s using external modulation of a DFB laser.....	28
Figure 3.1	Simulation block diagram for a lightwave system with a cascade of randomly misaligned multiplexers and demultiplexers.....	42
Figure 3.2	Time average spectrum of a MQW-DFB laser directly modulated at 2.5 Gb/s. The transmittance characteristic of a third-order Butterworth filter is also shown.....	43
Figure 3.3	The transmittance characteristic of a multi-layer dielectric film optical (de)multiplexer.....	44
Figure 3.4	Laser spectrum misalignment relative to the center frequency of the effective passband of the uniformly distributed concatenated multiplexers and demultiplexers.....	45

Figure 3.5a	Received eye-diagram at 10 Gb/s for lightwave systems with no optical filters.....	46
Figure 3.5b	Received eye-diagram at 10 Gb/s for lightwave systems with 30 uniformly distributed (de)multiplexers modeled as third-order Butterworth filters and ± 38 GHz laser misalignment.....	47
Figure 3.5c	Received eye-diagram at 10 Gb/s for lightwave systems with 30 uniformly distributed (de)multiplexers modeled as first-order Butterworth filters and ± 24 GHz laser misalignment.....	48
Figure 3.6a	System excess loss plus distortion-induced eye-closure penalty versus laser misalignment for a WDM network with 30 uniformly distributed (de)multiplexers.....	49
Figure 3.6b	Distortion-induced eye-closure penalty versus laser misalignment for a WDM network with 30 uniformly distributed (de)multiplexers.....	50
Figure 4.1	Simulation block diagram for a lightwave system with a cascade of randomly misaligned multiplexers and demultiplexers.....	60
Figure 4.2	The transmittance characteristic of a multi-layer dielectric film optical (de)multiplexer.....	61
Figure 4.3	Received eye-diagram at 0.3 dB distortion-induced eye-closure penalty for lightwave systems modulated at 10 Gb/s with 100 randomly misaligned (de)multiplexers modeled as third-order Butterworth filters and ± 18 GHz laser misalignment.....	62

Figure 4.4	Laser misalignment tolerances versus number of perfectly aligned and randomly misaligned (de)multiplexer cascades for a WDM optical network operating at 10 Gb/s per optical channel.....	63
Figure 4.5a	The effective transmittance characteristic of perfectly aligned 2(de)multiplexers in cascade (1 network element).....	64
Figure 4.5b	The effective transmittance characteristic of perfectly aligned 100 (de)multiplexers in cascade (50 network element).....	65
Figure 4.6	Laser misalignment tolerances versus number of randomly misaligned (de)multiplexers in cascade for a WDM optical network operating at either 2.5 Gb/s or 10 Gb/s per optical channel.....	66
Figure 5.1	Comparison of the theoretical and experimental multiplexer magnitude of the transfer function of a phased-array optical (de)multiplexer.....	71
Figure 5.2	Received eye-diagrams at 10 Gb/s per optical channel for a WDM optical network with a cascade of 8 multiplexers and 8 demultiplexers.....	72
Figure 5.3	Distortion-induced eye-closure penalty versus laser frequency misalignment for a WDM optical network operating at 10 Gb/s per optical channel with a cascade of 8 multiplexers and 8 demultiplexers.....	73

- Figure 6.1** Simulation block diagram for a lightwave system where the effective transfer function of the (de)multiplexer cascade is represented by an equivalent filter.....83
- Figure 6.2** A contour at 0.3 dB distortion-induced penalty for all possible combinations of the normalized magnitude coefficients m_1 (X – axis), and m_2 (Y – axis). The figure illustrates an example for a cascade of 30 (de)multiplexers modeled as 3rd-order Butterworth filters with operation at 10 Gb/s and at 2.5 Gb/s per optical channel. The intersections of the contour and the normalized coefficients for the two bit rates give the allowable laser misalignment tolerances.....84
- Figure 6.3** Distortion-induced eye-closure penalty versus normalized dispersion-like coefficient β_285

Chapter 1

Introduction

1.1 Multiwavelength Optical Networks: Definitions and Motivations

The field of optical communications has been and is still growing rapidly since the proposal of Kao and Hockham [1] to use glass fibers as a waveguide medium for optical communications in 1966. The main problem was the high loss of optical fibers; fibers available during the 1960's has losses in excess of 1000 dB/km. A breakthrough occurred in 1970 when Kapron, Keck, and Maurer reported a (monomode) quartz fiber with 20 dB loss per kilometer "within fifteen years fiber losses had been reduced below 0.2 dB/km" in the wavelength region near 1 μm [2]. At about the same time, GaAs semiconductor lasers, operating continuously at room temperature, were demonstrated [3]. the simultaneous availability of a compact optical source and a low-loss optical fiber led to a worldwide effort for developing fiber-optic communication systems. The capacity of a communication system can be measured by the bit rate-distance product BL , where B is the bit rate and L is the repeater spacing. Figure 1.1 shows the progress in the performance of lightwave systems realized after 1974 [4]. The progress has been rapid by several orders of magnitude increases in the bit rate-distance product over a period of less than 20 years.

An attractive technology option to utilize the vast bandwidth offered by the fiber is

by using the wavelength as an additional degree of freedom to transmit different channels in parallel on the same fiber. At the receiver different methods may be used to separate the individual channels again. A coherent transmission scheme [5] mixes the incoming signal with a local oscillator signal and provides the highest sensitivity and theoretically the most efficient usage of the available bandwidth. However, the complexity of coherent receivers and the stringent requirements on the stability of the local oscillator makes it unlikely that they will soon become commercialized.

An alternative concept is a Wavelength Division Multiplexed (WDM) direct detection system. WDM has been studied intensively as a technology option to create powerful and reliable telecommunication transport networks that allow graceful network evolution. WDM technologies may provide a number of benefits to local exchange and interexchange networks including: increased transport capacity [6] and flexibility [7], [8]; reduced equipment cost [9]; and enhanced network integrity [10]. Compared with all-optical multigigabit-per-second time-division multiplexing/demultiplexing schemes, WDM systems do not need clock synchronization, or clock recovery. With the commercial availability of Erbium-doped fiber amplifiers (EDFAs), WDM is expected to emerge from the laboratory to practical and widespread system applications.

EDFAs can ease constraints on system design because its broad spectrum provides the amplification gain required to compensate for the insertion loss caused by multiplexing components and power-dividing devices.

Multiplexers “for spatial combination of different channels” and demultiplexers “for spatial separation of different channels” are key components in WDM networks. As an example, in a WDM ring network [6], optical signal processing via WDM demultiplexing and multiplexing is used, to avoid electronic processing of digital signals that pass through an office, to drop and add primarily the traffic originating and terminating at each office. A liquid crystal Fabry-Perot (F-P) interferometer optical filter has been used as a (de)multiplexer [11]. Multi-layer dielectric film optical filters have also been used as (de)multiplexers [12]. Phased-array wavelength (de)multiplexers based on the principle of split, shift, and add using an array of curved waveguides are another important technology option for multiwavelength optical networks [13], [14], [15].

In a WDM optical network, every optical channel uses a dedicated laser source. Laser arrays are considered attractive light sources for use in WDM optical networks. WDM is essentially a parallel technology, and the use of array transmitters and receivers is intended to overcome the cost factors associated with the use of discrete devices, one per channel, in a natural and practical way [16].

Two key WDM components, namely, (de)multiplexers and transmitters, have significant effect on the performance of WDM networks. The following two sections provide description for each of them.

1.2 Optical Transmitter

The design of a multi-channel communication system requires careful consideration of the transmitter characteristics [17]. In a WDM system, every optical channel must have a dedicated laser and associated electronics, even in the case of a laser array. The operating characteristics, the stability, and the control of each of the optical carriers are important because the individual optical channels may be separated by only a few nanometers.

The emission spectrum of a laser source can change considerably over time due to change in the operating conditions such as temperature, humidity, and material aging. While such frequency changes may be of concern in a single-channel communication system, the carrier frequencies in a multi-channel system can be of far greater concern. This is because they must remain stable in both a relative sense so that channel spacing does not fluctuate with time, and individually so that the cumulative drifts of all of the network elements within a channel, including the transmitter, receiver, and WDM devices, do not inhibit transmission. For example, a Distributed Feedback (DFB) semiconductor laser used as single-longitudinal source will typically drift on the order of 0.1 to 0.15 nm/°C. This implies that a ThermoElectric Cooler (TEC) will likely be required to stabilize the junction temperature of the laser. Because the temperature sensor used in the control circuit of the TEC does not typically measure the junction of the laser, but rather some

point near the laser, it can be difficult to accurately maintain the laser's junction temperature during rapid changes in ambient temperature and over the lifetime of the device.

Direct current modulation of the laser signal causes substantial broadening and wavelength shifting within the inherent linewidth. This phenomena, referred to as optical frequency chirp, is of particular concern in high speed systems. Changing the current to perform the modulation causes changes in the index of refraction of the laser medium which, in turn, cause chirping. This condition can result in a chirp-induced dispersion penalty that can be severe for 10 Gb/s systems and can also affect the performance of a WDM system.

1.3 Optical Multiplexers and Demultiplexers

In a WDM network, the lightwave signal passes through a number of concatenated components, such as multiplexers, demultiplexers, EDFAs, and noise-limiting optical bandpass filters, all of which can serve as optical filters. The effect is a potentially significant narrowing of the effective passband.

Concatenation of components makes the system susceptible to passband misalignments arising from device imperfections and temperature variations. This also leads to narrowing the effective passband.

The purpose of this thesis is to evaluate the performance degradation of multiwavelength optical networks, due to laser and optical (de)multiplexer misalignment. The performance evaluation will cover point-to-point WDM optical

networks with a multiplexer and demultiplexer and optical networks with large number of (de)multiplexer cascades. The study also includes a comparison between simulation and experimental results for a WDM optical network with a cascade of 8 multiplexers and 8 (de)multiplexers. We also formulated a (de)multiplexer model that is general for any bit rate, any filter shape, any filter phase, and for any filter bandwidth. Since a cascade of (de)multiplexers is another multiplexer with effective magnitude equal to the product of all the magnitudes of the multiplexers in the cascade, and the effective phase is the sum of all the phases in the cascade, this model is also general for any number of (de)multiplexers in a cascade.

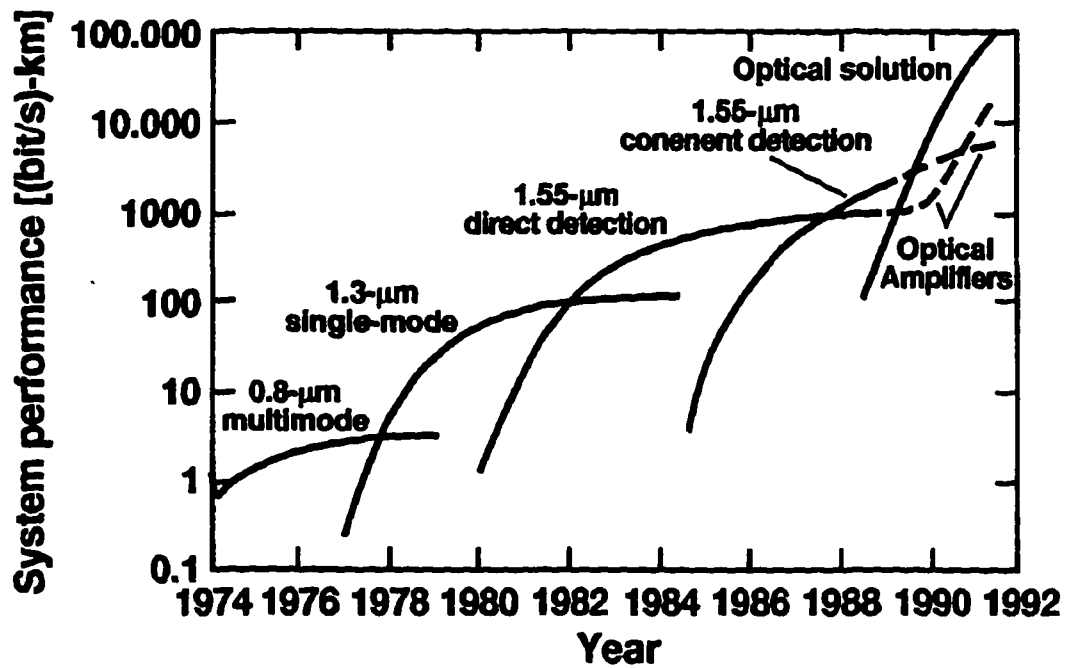


Figure 1.1: Progress in lightwave communication technology over the period 1974-1992. Different curves show the increase in the bit rate-distance product for five generations of fiber-optic communication systems.

Chapter 2

Performance Degradations of WDM Systems due to Laser and Optical Filter Misalignments at 1 dB System Excess Loss Criteria

2.1 Introduction

Wavelength division multiplexing (WDM) techniques are considered an attractive technology option for utilizing the vast bandwidth offered by optical fibers in optical Multiplexers networks [6], [7], [18]. In an optical network, the lightwave signal passes through a number of concatenated components, such as multiplexers (MUX), demultiplexers (DEMUX), EDFAs, and noise limiting optical bandpass filters, all of which can serve as optical filters. The concatenation of optical filters makes the system susceptible to filter passband misalignments arising from device imperfections, temperature variations, and aging. The emission spectrum of the laser source may also be misaligned with the effective center frequency of the optical filters due to manufacturing tolerances, aging, or operating conditions. Performance degradation in WDM systems may arise due to the combined effects of optical filter misalignments, laser misalignments, and laser chirp.

Previous work focused on a multi-channel star optical network architecture to determine the performance degradation due to the combined effect of laser chirp

and, using a single multiple-path interferometer filter (specifically, a Fabry-Perot filter), which has been modeled as a first order filter [19].

In this chapter, we use computer simulation techniques to evaluate the performance degradation for:

A) a single path of an interoffice WDM network using a cascade of two grating-based WDM optical filters (a multiplexer and a demultiplexer), taking into consideration misalignments between the two WDM optical filters, laser misalignments, and laser chirp [20]. The results are also compared to the case of using a cascade of either two multiple-path interferometer optical filters, or two multi-layer dielectric film optical filters.

B) WDM optical networks with large number of optical filters. In contrast to the multiple-path interferometer optical filters, which are modeled as first order filters, each of the grating-based WDM optical filters is modeled as a second order Butterworth filter, in agreement with experimental measurements [21]. The multi-layer dielectric film optical filters have been used in a multiwavelength network testbed [12], and are modeled as third order Butterworth filters in agreement with experimental measurements for their transmission characteristics. For lightwave systems using WDM technology with 2-nm or more channel spacing, the crosstalk is small enough to be neglected in this study.

2.2 The System Model

We model system "A" as a single path in an interoffice WDM network, and system "B" as a WDM optical network with large number of optical filters, both at 2.5

Gb/s and 10 Gb/s per optical channel. The path in system “A” consists of a transmitter, a multiplexer, a demultiplexer and a receiver, as shown in Fig.2.1. The simulation block diagram for system “B” consists of a transmitter, a cascade of optical filters and a receiver as shown in Fig. 2.2. At 2.5 Gb/s, two cases were considered: direct current modulation of a Multi-Quantum-Well Distributed Feedback laser (MQW-DFB) and direct current modulation of a bulk DFB laser. At 10 Gb/s two other cases were considered: direct modulation of a MQW-DFB laser, and external modulation of a DFB laser. The single-longitudinal -mode rate equations that describe the laser dynamics are expressed by:

$$\frac{dN}{dt} = \frac{I}{qV} - \frac{N}{\tau_n} - g(N - N_t) \frac{S}{1 + \epsilon S} \quad (2.1)$$

$$\frac{dS}{dt} = \Gamma g(N - N_t) \frac{S}{1 + \epsilon S} - \frac{S}{\tau_p} + \Gamma \beta \frac{N}{\tau_n} \quad (2.2)$$

Where N is the electron density, S is the photon density, Γ is the optical confinement factor given by the ratio of the active region volume to the modal volume, g is the gain slope constant, N_t is the electron density at which the net gain is zero, τ_p is the photon life time, τ_n is the electron life time, β is the fraction of the spontaneous emission coupled into the laser mode, V is the volume of the active layer, q is the electronic charge, ϵ is the gain compression factor, and I is the current injected into the active layer. Typical single-mode semiconductor laser parameter values [21] for both the Bulk DFB laser and the MQW-DFB laser used in this study are given in Table 2.1. A non return-to-zero (NRZ) random data length equal to 128 bits is used. The bias current I_b is assumed to be equal to the laser

threshold current I_{th} and the modulating current varies from 0 to $2I_{th}$. The laser-drive circuit is modeled as a simple RC circuit ($RC=21\text{psec}$). The electric field at the output of the laser facet (input to the multiplexer-demultiplexer cascade) is expressed by:

$$E_{in}(t) = \sqrt{P(t)} \exp[j2\pi \int_0^t f(\tau) d\tau], \quad (2.3)$$

where the output power per facet P is given by:

$$\frac{SV\eta hf}{2\Gamma\tau_p}, \quad (2.4)$$

and the laser instantaneous frequency (chirp) $f(t)$ is given by the relation:

$$\varphi(t) = 2\pi \int_0^t f(\tau) d\tau = -\int_0^t \left(\frac{1}{2}\right) \alpha \Gamma g \Delta N d\tau, \quad (2.5)$$

here, ΔN is the incremental carrier density, α is the linewidth enhancement factor, and η is the quantum efficiency,

and α is the linewidth enhancement factor. For externally-modulated systems, where the chirp is zero, the electric field input to the multiplexer-demultiplexer cascades is given by:

$$E_{in}(t) = \sqrt{P_{ext}(t)} \quad (2.6)$$

where $P_{ext}(t)$ is the output power from the external modulator simulated as a NRZ random data sequence of length equal to 128 bits. The FWHM for each optical filter is assumed to be 1 nm and is found to be much wider than the laser spectrum under modulation at 2.5 Gb/s and at 10 Gb/s. The receiver electrical filter is modeled as a third order Butterworth filter with 3 dB bandwidth of 0.65 times the bit rate.

The system excess loss versus the laser misalignments (Δf) is calculated relative to the case without optical filters for different values of the optical filter misalignments (δf). Here, Δf is the difference between the center frequency of the laser spectrum under modulation and the center frequency of the effective passband of the concatenated multiplexer and demultiplexer, and δf is the absolute difference between the center frequencies of the MUX and the DEMUX, as shown in Fig. 2.3.

The system excess loss is equal to $10 \log \frac{a}{b}$, where a is the average received optical power for a WDM system without optical filters, and b is the average received optical power for the WDM system under study. Minimum system excess loss occurs when the center frequency of the laser spectrum under modulation coincides with the center frequency of the effective passband of the concatenated multiplexer and demultiplexer.

2.3 Simulation Results for a Cascade of a Multiplexer and a Demultiplexer

At 2.5 Gb/s per optical channel, the system excess loss is almost the same for either direct modulation of a MQW-DFB laser, or direct modulation of a Bulk DFB laser. With a MQW-DFB laser, laser misalignments of ± 35 GHz for 25 GHz optical filter misalignments produce 1 dB system excess loss. However, 75 GHz filter misalignments produce 1 dB system excess loss if the center frequency of the laser spectrum under modulation is perfectly aligned with the center frequency of the effective passband of the concatenated multiplexer and demultiplexer as shown in Fig.2.4. With a Bulk DFB laser misalignments of ± 33 GHz for 25 GHz optical filter misalignments produce 1 dB system excess loss and, as before 75 GHz filter

misalignments produce 1 dB system excess loss if the center frequency of the laser spectrum is perfectly aligned as shown in Fig.2.5.

At 10 Gb/s per optical channel, the system excess loss is calculated for two cases: direct current modulation of a MQW-DFB laser and external modulation, which are considered attractive options at this bit rate. For the case using MQW-DFB laser, laser misalignments of ± 29 GHz for 25 GHz optical filter misalignments produce 1 dB system excess loss as shown in Fig. 2.6. With external modulation laser misalignments of ± 33 GHz for 25 GHz optical filter misalignments produce 1 dB system excess loss. In both cases 75 GHz filter misalignments produce 1 dB system excess loss if the laser spectrum under modulation is perfectly aligned with the passband of the concatenated MUX and DEMUX as shown in Fig. 2.7.

Table 2.2 summarizes the required misalignment tolerances at 1 dB system excess loss for WDM systems using all three types of optical filters: two grating-based optical filters, two multiple-path interferometer optical filters, or two multi-layer dielectric film optical filters. Comparing laser and optical filter misalignments tolerances, systems using two multiple-path interferometer optical filters require more stringent control of misalignments than systems using two grating-based optical filters. Systems using two multi-layer dielectric film optical filters require the least stringent control of misalignments compared to either systems using two grating-based optical filters or systems using two multiple-path interferometer optical filters.

2.4 Conclusions for a Cascade of a Multiplexer and a Demultiplexer

Using computer simulation techniques, we evaluate the limitations on laser and optical filter misalignments for various modulation techniques, at different bit rates, using either two multiple-path interferometer optical filters, two grating-based optical filters, or two multi-layer dielectric film optical filters. The results are significantly dependent on the type of the optical filters used. WDM systems at 1 dB system power excess loss for 25 GHz filter misalignments tolerate a laser misalignment of about ± 20 GHz using two multiple-path interferometer optical filters, ± 30 GHz using two grating-based optical filters, and ± 38 GHz using two multi-layer dielectric film optical filters. A 1 dB excess loss occurs when the center frequency of the laser under modulation is perfectly aligned with the center frequency of the effective passband of the optical filters for optical filter misalignments of 45 GHz using two multiple-path interferometer optical filters, 75 GHz using two grating-based optical filters, and 90 GHz using two multi-layer dielectric film optical filters. In this study the modulation speed and techniques are not an issue since the FWHM for each optical filter is much wider than the optical spectrum under modulation.

2.5 Simulation Results for a Cascade of Large Number of Multiplexers and Demultiplexers

At 2.5 Gb/s per optical channel, and for each case of cascading 10, 20, or 30 filters, laser misalignments tolerances are the same, for either using direct current modulation of a MQW-DFB laser, or direct current modulation of a Bulk DFB

laser. At 1dB system excess loss, with a cascade of 10 multiple-path interferometer optical filters, laser misalignment tolerances are ± 10 GHz, with a cascade of 20 multiple-path interferometer filters, laser misalignment tolerances are ± 7 GHz, and with a cascade of 30 multiple-path interferometer filters, laser misalignment tolerances are ± 5 GHz. However, for the case where the center frequency of the laser spectrum is perfectly aligned with the center frequency of the effective passband of the concatenated filters, using MQW-DFB laser, a cascade of 700 multiple-path optical filters produce 1 dB system excess loss. Using Bulk DFB lasers, where the chirp has clear effect on the laser spectrum such that the laser spectrum under modulation is wider than the spectrum of a MQW-DFB laser as shown in Fig. 2.8 and Fig. 2.9, the number of optical filters in a cascade falls to 350 multiple-path interferometer optical filters to produce 1 dB system excess loss if the center frequency of the laser spectrum is perfectly aligned with the center frequency of the effective passband of the optical filters.

At 10 Gb/s per optical channel, the system excess loss is calculated for either using direct current modulation of a MQW-DFB laser or using external modulation. For the case using direct current modulation of MQW-DFB laser, with a cascade of 10 multiple-path interferometer optical filters, even with the laser spectrum under modulation is perfectly aligned with the effective passband of the concatenated optical filters, the system excess loss is more than 1 dB, this is because the chirp has greater effect at 10 Gb/s than at 2.5 Gb/s as shown in Fig. 2.10 and Fig. 2.11. However using external modulation, where the chirp is not a problem, it takes a

concatenation of 100 multiple-path optical filters to produce 1 dB system excess loss if the laser spectrum under modulation is perfectly aligned with center frequency of the effective passband of the cascaded filters. Therefore it was possible it was possible using external modulation technique to concatenate 10, 20, and 30 multiple-path interferometer optical filters. The laser misalignment tolerances at 1 dB system excess loss are : ± 10 GHz for the case of cascading 10 multiple-path interferometer optical filters, it is ± 7 GHz if 20 multiple-path interferometer optical filters are cascaded, and it is ± 5 GHz if 30 multiple-path filters are cascaded. Even with the fact that the chirp is not an issue, still the spectrum of the laser under modulation at 10 Gb/s using external modulation technique is wider than the spectrum of the laser spectrum using direct modulation of MQW-DFB laser at 2.5 Gb/s.

Table 2.3 summarizes the required laser misalignment tolerances for WDM systems for the cases with either 10, 20, or 30 optical filters, using all three types of optical filters: multiple-path interferometer optical filters, grating-based optical filters, or multi-layer dielectric film optical filters. Comparing laser misalignment tolerances for each case of 10, 20, or 30 optical filters, systems using multiple path interferometer optical filters require more stringent control of laser misalignment than systems using grating-based optical filters. Systems using multi-layer dielectric film optical filters require the least stringent control of misalignments compared to systems using either grating-based optical filters or systems using multiple-path interferometer optical filters.

2.6 Conclusions for a Cascade of Large Number of Optical filters

In this section, we use computer simulation techniques to evaluate the limitations on laser misalignments for various modulation techniques, at different bit rates, using either multiple-path interferometer optical filters, grating-based optical filters, or multi-layer dielectric film optical filters, for the cases of cascading 10, 20, or 30 filters. The results are significantly dependent on the type of the optical filters used. If grating-based or multi-layer optical filters are used, the modulation technique and the bit rate are not significant factors. At 1 dB system excess loss, at 2.5 Gb/s using direct current modulation of either MQW-DFB laser or Bulk DFB laser, or at 10 Gb/s using either direct current modulation of MQW-DFB or external modulation, the laser misalignments are: ± 25 GHz if 10 grating-based optical filters are cascaded, ± 21 GHz if 20 grating-based optical filters are cascaded, and ± 19 GHz if 30 grating-based optical filters are cascaded. Laser misalignment tolerances are: ± 34 GHz if 10 multi-layer dielectric film optical filters are cascaded, ± 31 GHz if 20 multi-layer dielectric film optical filters are cascaded, ± 29 GHz if 30 multi-layer dielectric film optical filters are cascaded. The modulation techniques and/or the bit rate become significant factors if the type of the optical filters used are multiple-path interferometer. While at 10 Gb/s is not possible, even with the laser spectrum is perfectly aligned, to cascade 10 multiple-path interferometer using direct current modulation of MQW-DFB laser; it is possible to cascade 100 multiple-path optical filters if external modulation is used.

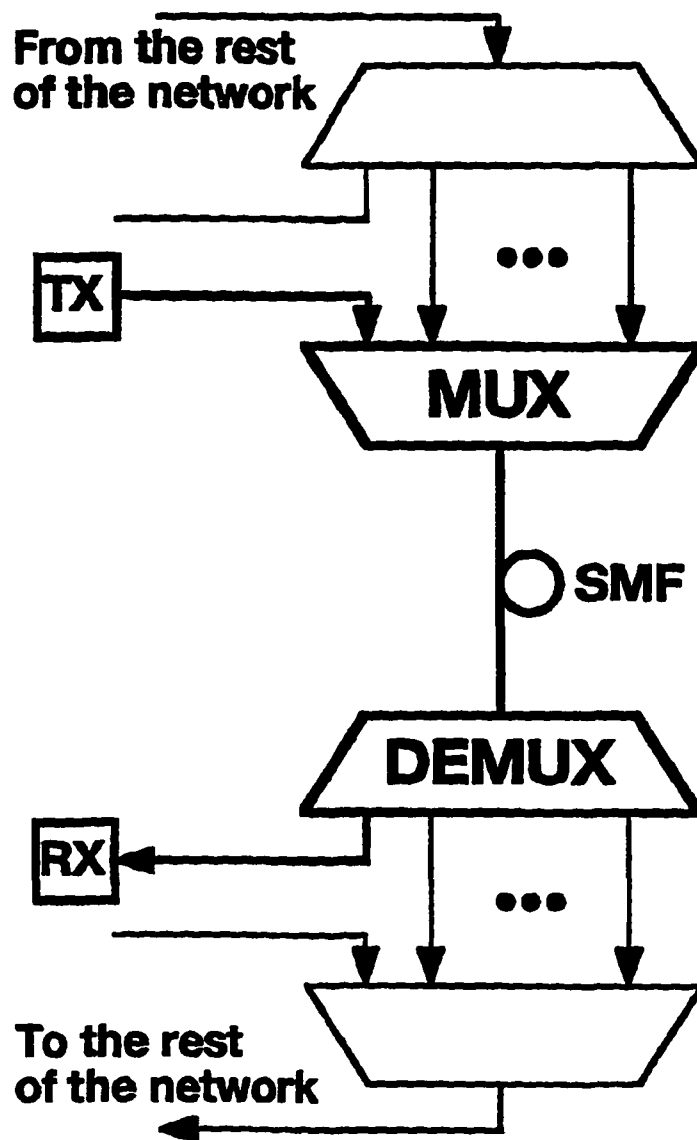
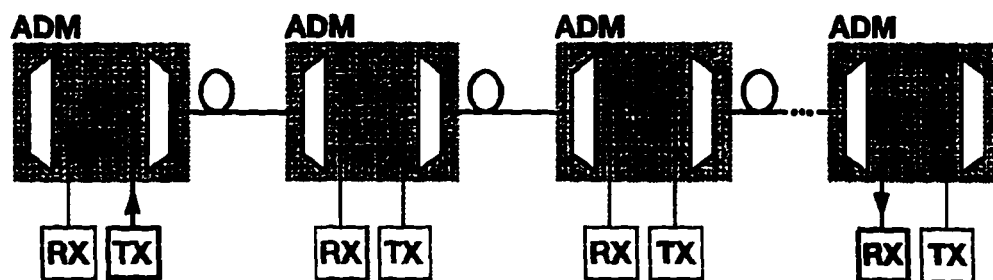


Figure 2.1: A Block diagram of typical WDM network architecture (system used in simulation is emphasized).



ADM = Add & Drop Multiplexer

Figure 2.2: Simulation block diagram for WDM system with a cascade of large number of multiplexers and demultiplexers.

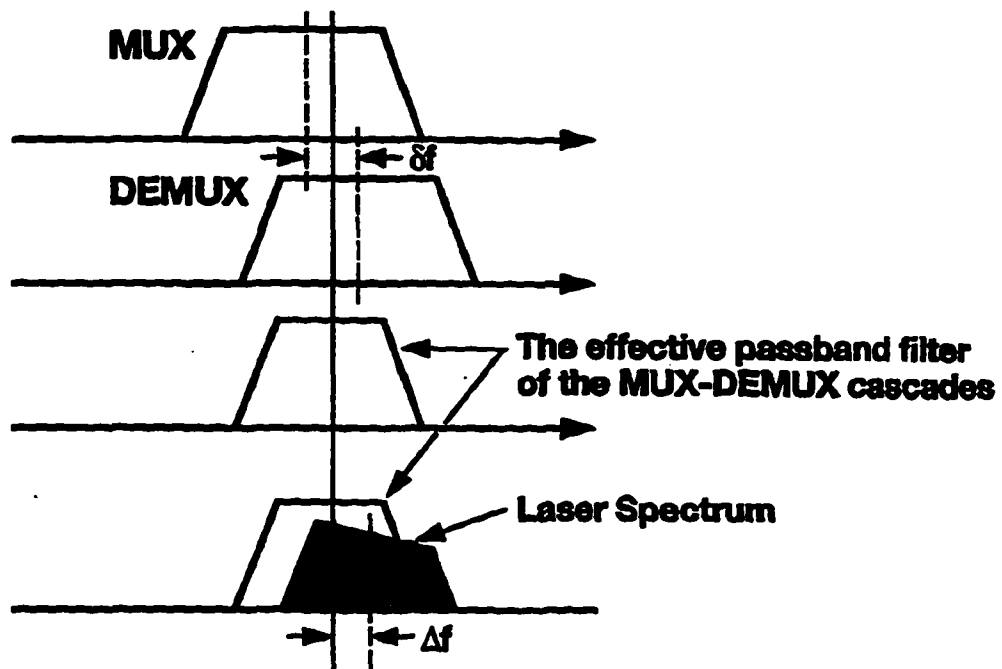


Figure 2.3: Laser spectrum and multiplexer/demultiplexer transmission characteristics.

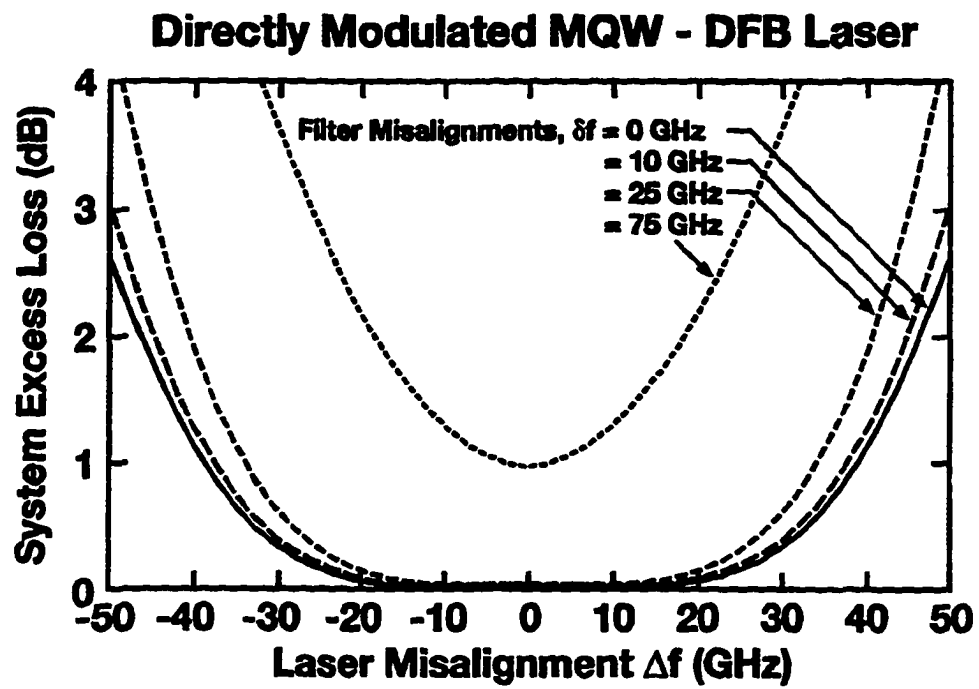


Figure 2.4: System excess loss at 2.5 Gb/s using direct current modulation of MQW-DFB laser.

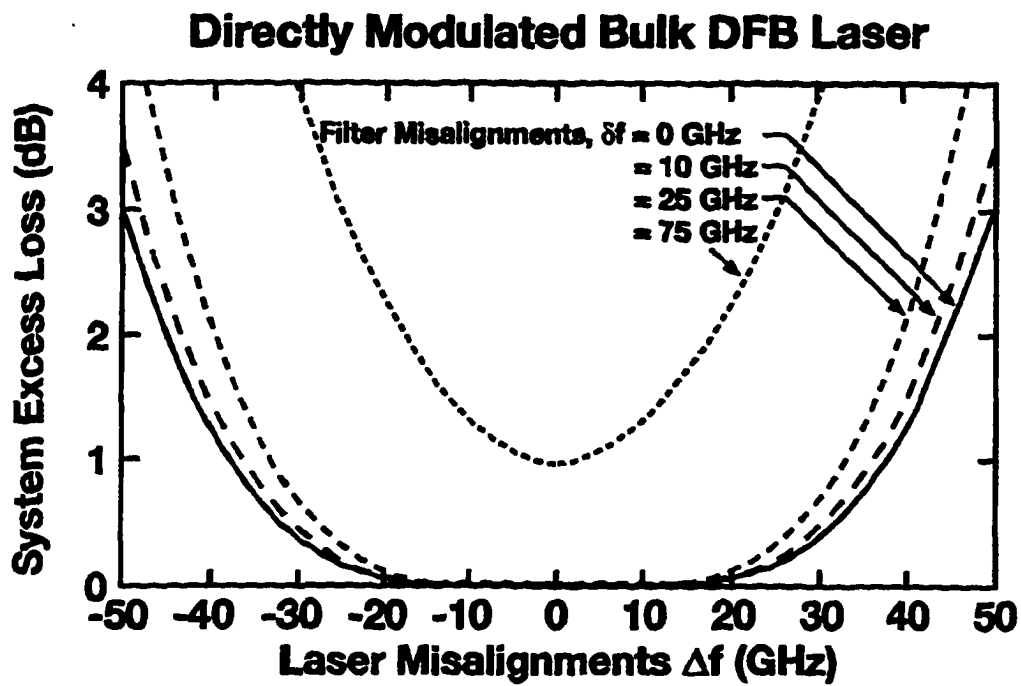


Figure 2.5: System excess loss at 2.5 Gb/s using direct current modulation of a Bulk-DFB laser.

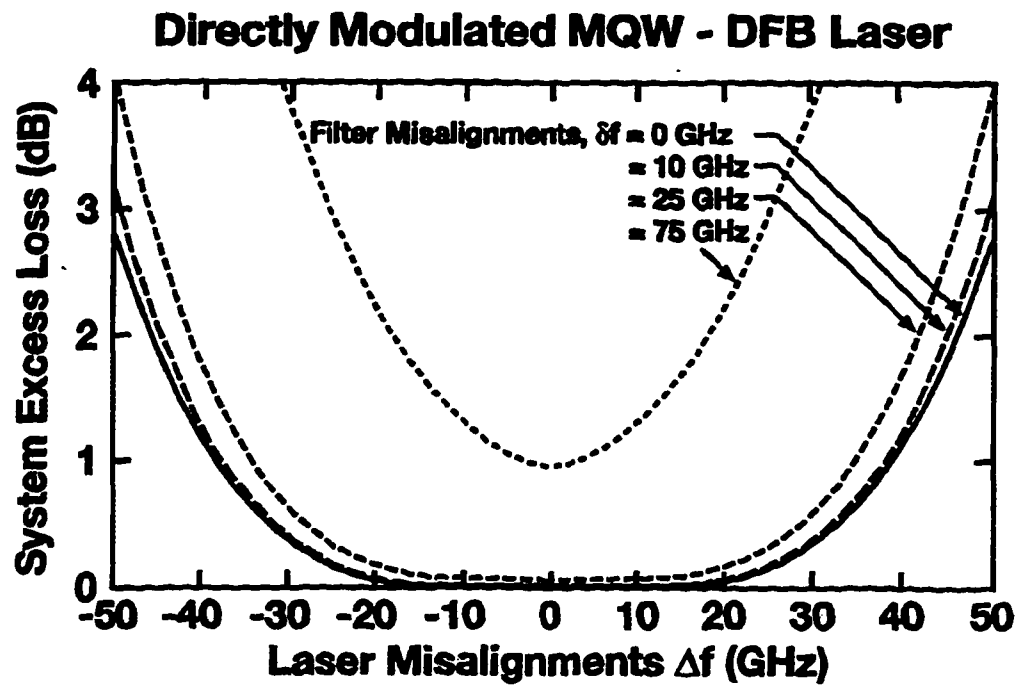


Figure 2.6: System excess loss at 10 Gb/s using direct current modulation of MQW-DFB laser.

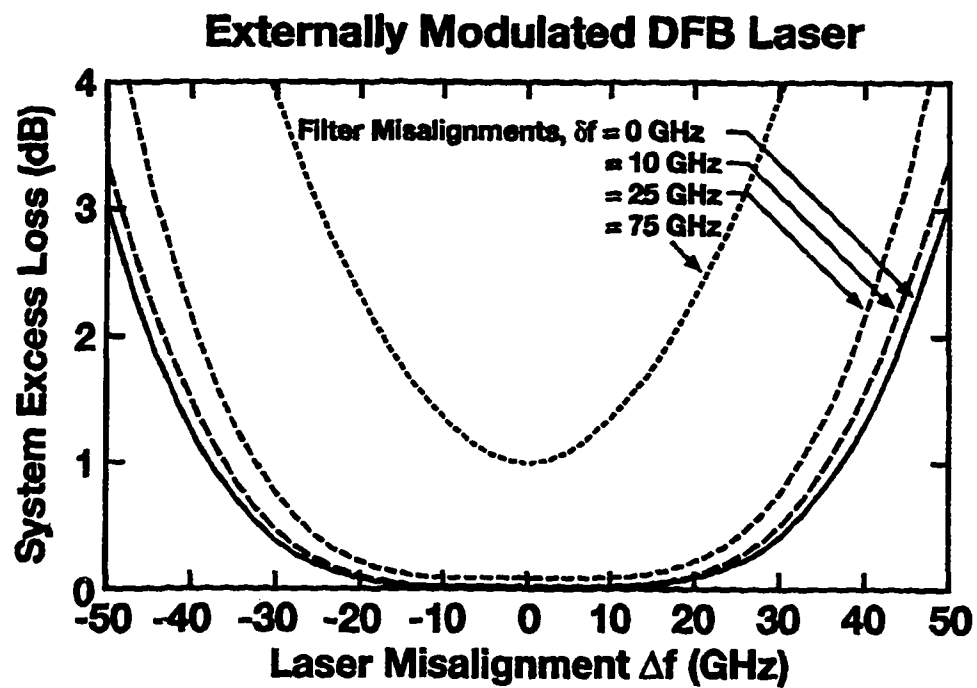


Figure 2.7: System excess loss at 10 Gb/s using external modulation of a Bulk-DFB laser.

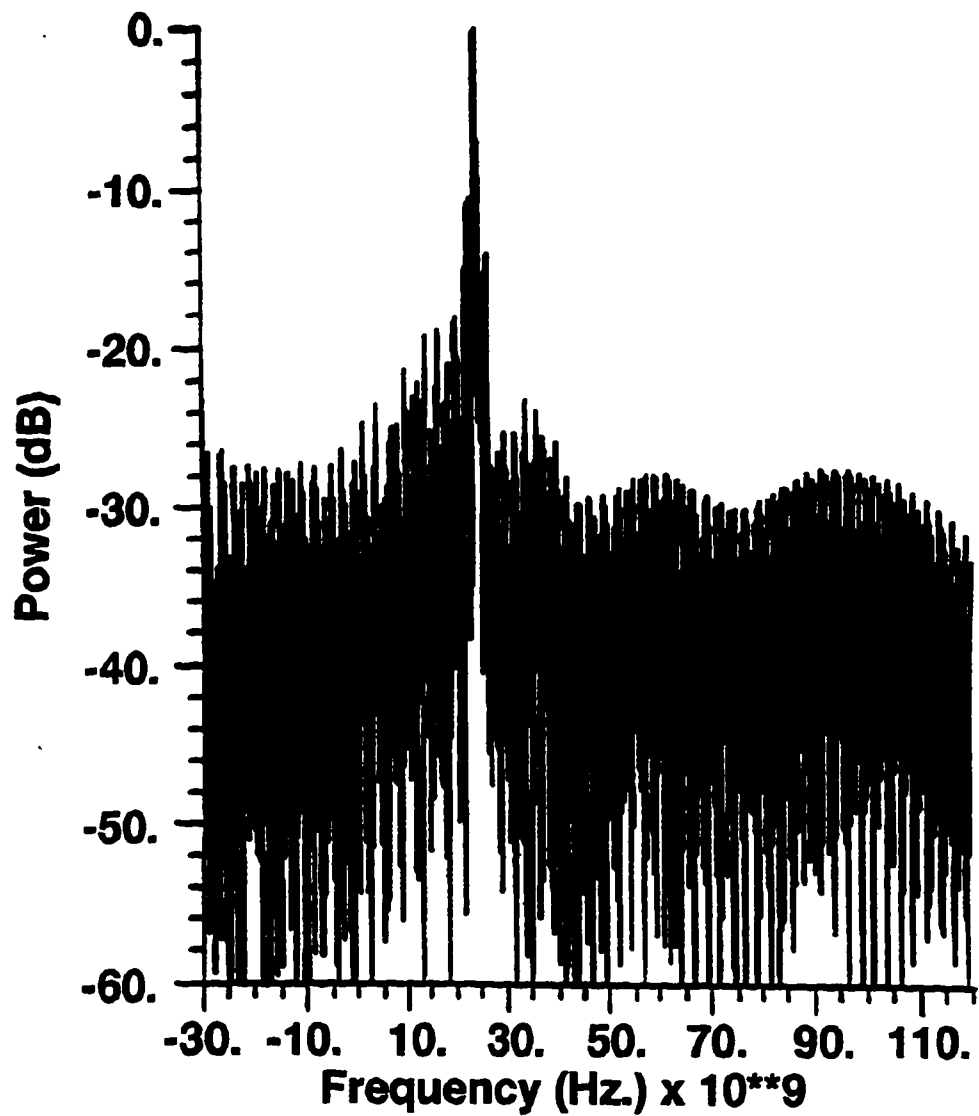


Figure 2.8: Laser spectrum under modulation at 2.5 Gb/s using direct current modulation of a Bulk-DFB laser.

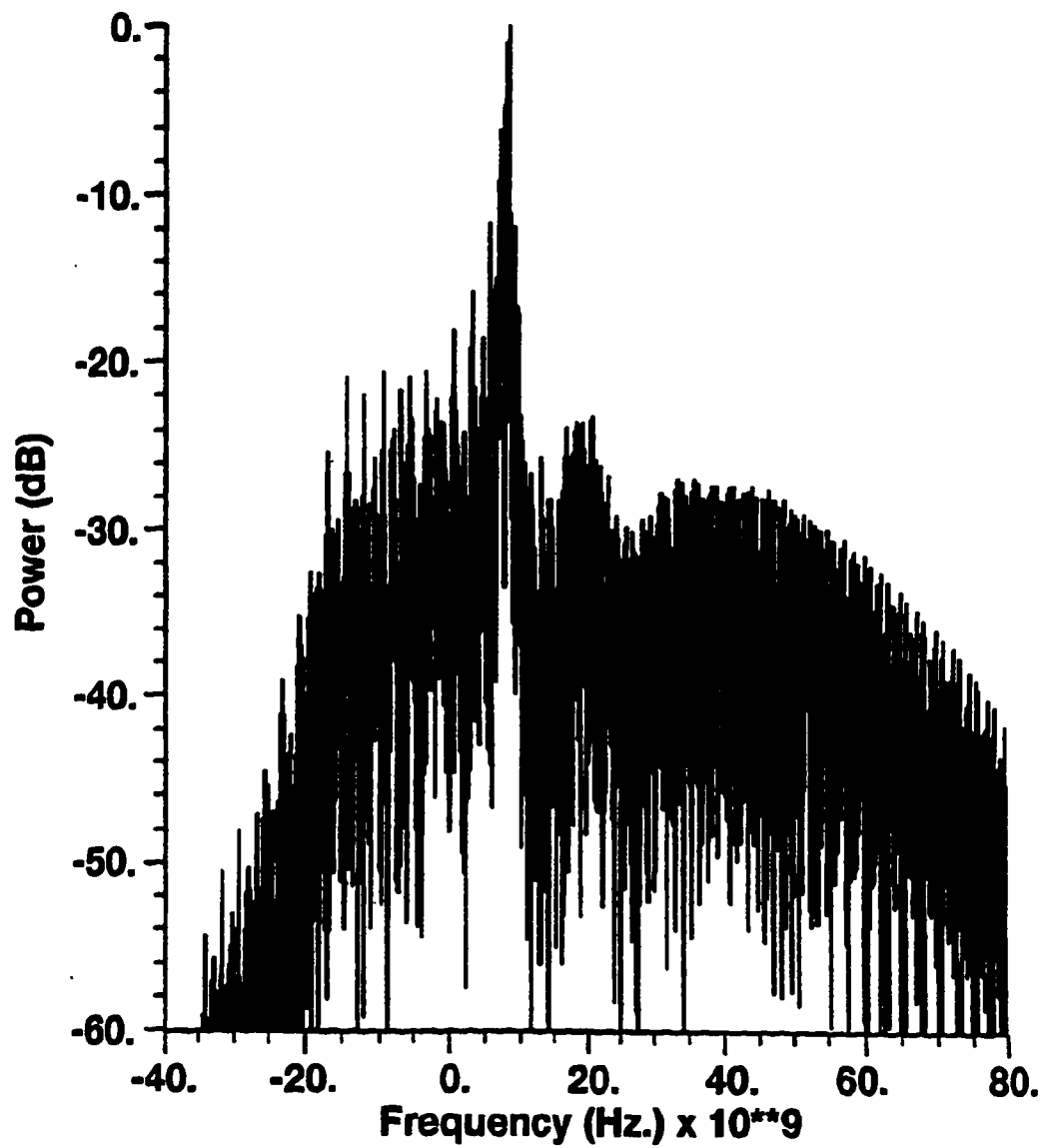


Figure 2.9: Laser spectrum under modulation at 2.5 Gb/s using direct current modulation of a MQW-DFB laser.

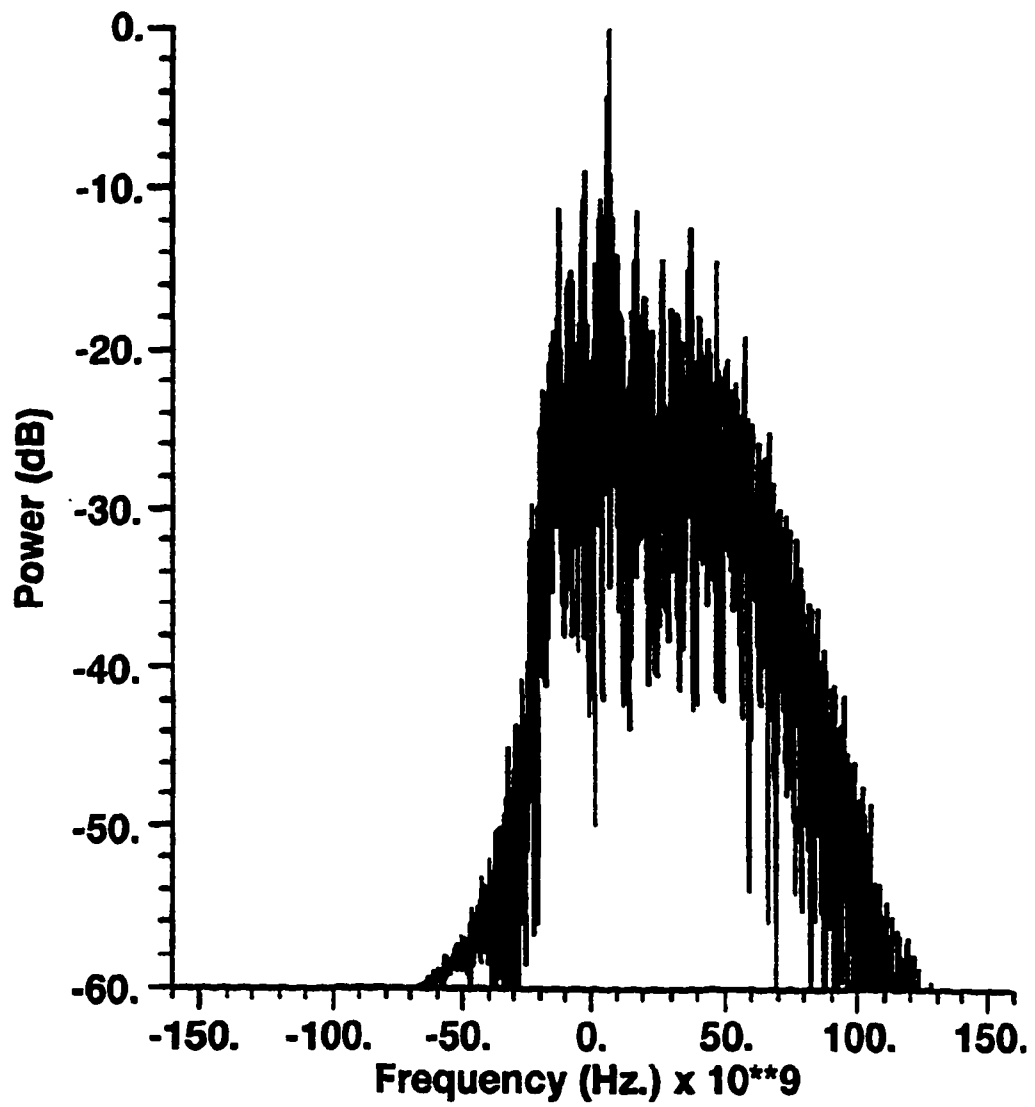


Figure 2.10: Laser spectrum under modulation at 10 Gb/s using direct current modulation of a MQW-DFB laser.

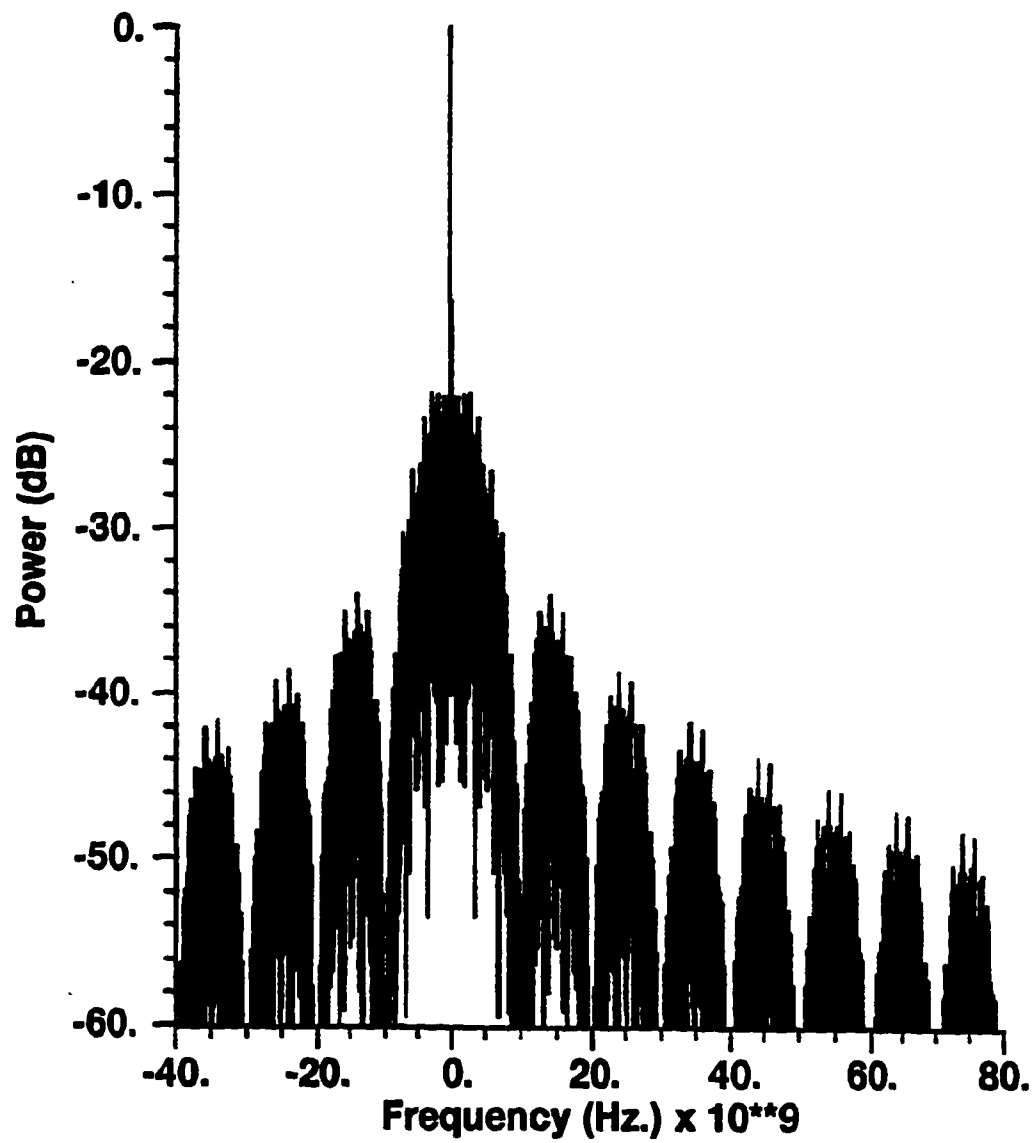


Figure 2.11: Laser spectrum under modulation at 10 Gb/s using external modulation of a DFB laser.

	Bulk DFB Laser	MQW-DFB Laser
Active-layer volume (m ³)	$v=4.5 \times 10^{-17}$	$v=2.1 \times 10^{-17}$
Spontaneous emission factor	$\beta=1.1 \times 10^{-4}$	$\beta=1.1 \times 10^{-4}$
Optical confinement factor	$\Gamma=0.28$	$\Gamma=0.085$
Optical gain constant (m ³ /sec)	$g=2.7 \times 10^{-12}$	$g=7.55 \times 10^{-12}$
Gain compression factor (m ³)	$\epsilon=2.5 \times 10^{-23}$	$\epsilon=5.0 \times 10^{-23}$
Linewidth enhancement factor	$\alpha=7.0$	$\alpha=3.5$
Transparency carrier density (m ⁻³)	$N_t=1.0 \times 10^{24}$	$N_t=1.2 \times 10^{24}$
Carrier lifetime (sec)	$\tau_n=0.5 \times 10^{-9}$	$\tau_n=0.5 \times 10^{-9}$
Photon lifetime (sec)	$\tau_p=1.0 \times 10^{-12}$	$\tau_p=1.5 \times 10^{-12}$
Quantum efficiency	$\eta=0.3$	$\eta=0.3$
Laser wavelength (m)	$\lambda=1.55 \times 10^{-6}$	$\lambda=1.55 \times 10^{-6}$

Table 2.1: Semiconductor laser parameter values used in solution of single-mode rate equations.

Bit Rate	Type of Modulation	WDM Filter Type	Filter Misalignments with a Perfectly Aligned Laser*	Laser Misalignments with 25 GHz Filter Misalignments*
2.5 Gb/s	MQW-DFB	Multiple-path interferometer	45 GHz	±22
2.5 Gb/s	Bulk-DFB	Multiple-path interferometer	45 GHz	±20
2.5 Gb/s	MQW-DFB	Grating-based	75 GHz	±35
2.5 Gb/s	Bulk-DFB	Grating-based	75 GHz	±33
2.5 Gb/s	MQW-DFB	Multi-layer dielectric film	90 GHz	±38
2.5 Gb/s	Bulk-DFB	Multi-layer dielectric film	90 GHz	±38
10 Gb/s	DFB-MQW	Multiple-path interferometer	45 GHz	±17
10 Gb/s	External	Multiple-path interferometer	45 GHz	±19
10 Gb/s	DFB-MQW	Grating-based	75 GHz	±29
10 Gb/s	External	Grating-based	75 GHz	±33
10 Gb/s	MQW-DFB	Multi-layer dielectric film	85 GHz	±38
10 Gb/s	External	Multi-layer dielectric film	90 GHz	±38

Table 2.2: Laser frequency misalignment tolerances for a point-to-point WDM systems with different types of optical filters.

Bit Rate	Type of Modulation	WDM Filter Type	Laser Misalignment with a cascade of 10 Optical Filters*	Laser Misalignment with a cascade of 20 Optical Filters*	Laser Misalignment with a cascade of 30 Optical Filters*	Max. # of cascade optical filters with a perfectly aligned laser*
2.5 Gb/s	MQW-DFB	Multiple-path interferometer	±10 GHz	±7 GHz	±5 GHz	700
2.5 Gb/s	Bulk-DFB	Multiple-path interferometer	±10 GHz	±7 GHz	±5 GHz	350
2.5 Gb/s	MQW-DFB	Grating-based	±25 GHz	±21 GHz	±19 GHz	>2000
2.5 Gb/s	Bulk-DFB	Grating-based	±25 GHz	±21 GHz	±19 GHz	>2000
2.5 Gb/s	MQW-DFB	Multi-layer dielectric film	±34 GHz	±31 GHz	±29 GHz	>2000
2.5 Gb/s	Bulk-DFB	Multi-layer dielectric film	±34 GHz	±31 GHz	±29 GHz	>2000
10 Gb/s	DFB-MQW	Multiple-path interferometer	**	**	**	8
10 Gb/s	External	Multiple-path interferometer	±10 GHz	±7 GHz	±5 GHz	100
10 Gb/s	DFB-MQW	Grating-based	±25 GHz	±21 GHz	±18 GHz	80
10 Gb/s	External	Grating-based	±25 GHz	±21 GHz	±19 GHz	1600
10 Gb/s	MQW-DFB	Multi-layer dielectric film	±34 GHz	±30 GHz	±28 GHz	115
10 Gb/s	External	Multi-layer dielectric film	±34 GHz	±31 GHz	±29 GHz	1750

*At 1 dB System excess loss

**System excess loss is higher than 1 dB

Table 2.3: Laser frequency misalignment tolerances for WDM systems using large number and different types of perfectly aligned optical filters

Chapter 3

Performance Degradation of Multiwavelength Optical Networks due to Laser and (De)multiplexer Misalignments for 30 (de)multiplexers in Cascade

3.1 Introduction

Wavelength division multiplexing (WDM) techniques are considered an attractive technology option for building a flexible optical network layer [6], [7], [18]. In a multiwavelength optical network, the lightwave signal passes through a number of concatenated components, such as WDM multiplexers, demultiplexers, EDFAs, and noise-limiting optical bandpass filters, all of which can serve as optical filters. The concatenation of optical filters makes the network susceptible to filter passband misalignments arising from device imperfections, temperature variations, and aging. Laser arrays are considered attractive light sources for use in multiwavelength optical networks. However, array technology provides less control of the laser wavelengths, relative to the effective center frequency of the concatenated optical filters, than discrete single-channel devices [24]. Furthermore, direct current modulation of a single-longitudinal-mode laser source introduces chirp, resulting in broadening of the modulation bandwidth of the optical spectrum.

Performance degradation in multiwavelength optical networks systems may arise due to the combined effects of optical filter misalignments, laser misalignment, and laser chirp.

In previous work, we have determined the system excess loss for a single path of an interoffice WDM network with two (de)multiplexers, taking into consideration misalignment between the two WDM optical filters (a multiplexer and a demultiplexer), laser misalignment, and laser chirp, [20], [23].

In this chapter we use computer simulation techniques to evaluate the performance degradation (in terms of the system excess loss and the system distortion-induced eye-closure penalty) of a multiwavelength optical network with a cascade of 30 randomly misaligned (de)multiplexers taking into consideration laser misalignment, and laser chirp. For lightwave systems using WDM technology with 200 GHz or more channel spacing, crosstalk is small enough to be neglected in this study. It also should be noted that a lightwave signal may pass through 15 network elements (i.e 30 (de)multiplexers) in a typical multiwavelength ring network [6].

3.2 The System Model

The simulation block diagram for the WDM system considered is shown in Fig.3.1. The system consists of a transmitter at 2.5 Gb/s or 10 Gb/s per optical channel, a cascade of randomly misaligned (de)multiplexers, and a receiver. At 2.5 Gb/s per optical channel, three cases are considered: direct current modulation of a Multi-Quantum-Well Distributed Feedback laser (MQW-DFB), direct current

modulation of a Bulk DFB laser and external modulation of a DFB laser. At 10 Gb/s per optical channel, external modulation of a DFB laser is considered. The dynamics of the DFB laser diode are modeled using the single-longitudinal-mode rate equations with laser parameters given in [22]. A non return-to-zero (NRZ) random data sequence of length equal to 128 bits is used. The bias current I_b is assumed to be equal to the laser threshold current I_{th} and the modulating current varies from 0 to $2I_{th}$. The laser-drive circuit is modeled as a simple RC circuit (RC=21 psec). The electric field at the output of the laser facet (input to the optical filter cascade) is expressed by:

$$E_{in}(t) = \sqrt{P(t)} \exp \left[j2\pi \int_0^t f(\tau) d\tau \right] \quad (3.1)$$

where $P(t)$ and $f(t)$ are the laser output power and the laser instantaneous frequency (chirp) respectively. For externally-modulated systems, where the chirp is zero, the electric field input to the optical filter cascade is given by:

$$E_{in}(t) = \sqrt{P_{ext}(t)} \quad (3.2)$$

Here, $P_{ext}(t)$ is the output power from the external modulator simulated as NRZ random data sequence of length equal to 128 bits.

The two types of the (de)multiplexers considered in the simulation are modeled as first-order and third-order Butterworth filters with filter transmittance characteristics given by:

$$H_B = \frac{1}{1 + \left[\frac{2(f - f_0 - \delta f)}{f_c} \right]^{2n}} \quad (3.3)$$

where f is the optical frequency, f_0 , is the center optical frequency of the optical filter, f_c is the FWHM which is assumed to be 125 GHz (1 nm), δf is the filter center frequency misalignment from f_0 and n is the order of the filter.

The theoretical filter shapes used in the simulation represent WDM (de)multiplexers technologies fairly well. For example, a liquid crystal Fabry-Perot (F-P) interferometer optical filter has been used as a (de)multiplexer [11] with transmittance characteristic that can be modeled as a first-order Butterworth filter. Alternatively, multi-layer dielectric film (de)multiplexers with FWHM equal to 312 GHz (2.5 nm) have been used in a multiwavelength network testbed [12]. The transmittance characteristic of each multi-layer dielectric (de)multiplexer is modeled as a third-order Butterworth filter in agreement with experimental measurements, as shown in Fig. 3.2. To incorporate the multi-layer dielectric film (de)multiplexer in the simulation model, the FWHM is scaled down from 312 GHz to 125 GHz, while retaining the assumption of a third-order Butterworth characteristic.

Phased-array wavelength (de)multiplexers based on the principle of split, shift, and add using an array of curved waveguides are another important technology option for multiwavelength optical networks [13], [14], [15]. The transmittance characteristics of phased-array (de)multiplexers may be modeled as second-order

Butterworth filters if the input optical signal is split into equal intensity components in each path with constant phase difference between the adjacent paths [15]. It may also be possible to design these types of (de)multiplexers with transmittance characteristics to fit Butterworth filters with order higher than two.

The passband of each (de)multiplexer used in the simulation, with FWHM=125 GHz, is found to be much wider than the spectrum of the laser under modulation at 2.5 Gb/s and 10 Gb/s as shown in Fig. 3.3.

Two cases are considered in the simulation. In the first case, the center frequencies of all cascaded (de)multiplexers are assumed to be perfectly aligned. In the second case, the cascaded (de)multiplexers are assumed to be uniformly misaligned over a range of up to ± 12.5 GHz as shown in Table 3.1. Because of the linearity of the system we are dealing with, the sequence of the misalignment of the (de)multiplexers in the system has no effect on the results.

A cascade of randomly misaligned (de)multiplexer has an effective passband narrower than the passband of each single (de)multiplexer and centered at optical frequency $f_{0_{\text{eff}}}$, which is not necessarily equal to f_0 . The laser misalignment (Δf) is defined as the difference between the center frequency of the laser spectrum under modulation and the center frequency of the effective passband of the concatenated (de)multiplexers $f_{0_{\text{eff}}}$ as shown in Fig. 3.4.

The receiver electrical filter is modeled as a third-order Butterworth filter with a 3

dB bandwidth equal to 0.65 times the bit rate in order to minimize the receiver noise while maximizing the eye opening.

The system excess loss and distortion-induced eye-closure penalty versus laser misalignment (Δf) are calculated relative to the case without (de)multiplexers. The system excess loss is caused by the optical signal being located on the edge of the filter and is equal to $10 \log \frac{a}{b}$, where a is the average received optical power for a system without (de)multiplexers, and b is the average received optical power for the WDM system under study. This is assumed to be equal to the ratio between the steady state signal level difference between logical ONE and logical ZERO calculated for a system without (de)multiplexers and for the WDM system under study. The distortion-induced eye-closure penalty for the WDM system under study is caused by the slope of the filter shape and is equal to $10 \log \frac{c}{d}$, where c is the steady-state signal level difference between logical ONE and logical ZERO, and d is the eye opening. Minimum system excess loss and distortion-induced penalty occur when the center frequency of the laser spectrum under modulation coincides with the center frequency of the effective passband of the concatenated (de)multiplexers.

In a multiwavelength optical network, the system excess loss can be overcome by optical amplifier gain. However, eye-closure penalty due to waveform distortion caused by the (de)multiplexer cascade is a fundamental limit and can not be eliminated.

3.3 Simulation Results

In a first set of simulation runs, the laser misalignment tolerances for 1 dB system excess loss are computed. This criteria produces very stringent misalignment tolerances, which are found to be almost the same for all modulation formats: at 2.5 Gb/s using either direct current modulation of a MQW-DFB laser, direct current modulation of a Bulk DFB laser, or external modulation of a DFB laser, and at 10 Gb/s using external modulation of a DFB laser. The results of the system excess loss do not depend on the modulation techniques and the bit rate. The results strongly depend on the type of the filters used. This is because the spectrum of the laser under modulation is much narrower than the passband of each filter used in this simulation with FWHM=125 GHz as shown in Fig. 3.3. With 30 perfectly aligned third-order Butterworth filters, laser misalignment tolerance is ± 29 GHz, and is ± 23 GHz if the filters are uniformly misaligned. With 30 perfectly aligned first-order Butterworth filters, the laser misalignment is ± 6 GHz. However, the system excess loss is higher than 1 dB if the (de)multiplexers are uniformly misaligned even when the center frequency of the laser spectrum under modulation is perfectly aligned with the center frequency of the effective passband of the (de)multiplexer cascade.

In a second set of simulation runs, a more relaxed criteria is examined, corresponding to 1 dB distortion-induced eye-closure penalty. Fig. 3.5 shows the received eye diagrams for a WDM system with a cascade of 30 uniformly misaligned filters using external modulation at 10 Gb/s per optical channel for

three cases. The received eye diagram for the case without optical filters is shown in Fig. 3.5a. The received eye diagram for a WDM system using third-order Butterworth filters with ± 38 GHz laser misalignment is shown in Fig. 3.5b, where the system excess loss is 10.2 dB and the distortion-induced eye-closure penalty is 1 dB. The received eye diagram for a WDM system using first-order Butterworth filters with ± 24 GHz laser misalignment is shown in Fig. 5c, where the system excess loss is 18.5 dB and the distortion-induced eye-closure penalty is 1 dB. Laser misalignment tolerances at 1 dB distortion-induced eye-closure penalty do not depend strongly on the bit rate and modulation techniques but strongly depend on the type of the filters used. At 2.5 GB/s per optical channel, laser misalignment tolerances vary from ± 41 GHz (for direct modulation) to ± 44 GHz (for external modulation) for systems using third-order Butterworth filters. Laser misalignment tolerances vary from ± 27 GHz (for direct modulation) to ± 30 GHz (for external modulation) for systems using first-order Butterworth filters.

Fig. 3.6 shows system excess loss and distortion-induced eye-closure penalty versus laser misalignment for 30 uniformly misaligned filters. Note that at 1 dB distortion-induced eye-closure penalty, the distortion curve is very steep and the corresponding eye diagrams are very poor (see Fig. 3.5). A more practical criteria occurs for 0.3 dB distortion-induced penalty, which is near the “knee” of the distortion curve where the eye diagrams still look good. Laser misalignment of ± 30 GHz produces 3.5 dB system excess loss and 0.3 dB distortion-induced penalty if third-order Butterworth filters are used. Multiwavelength optical

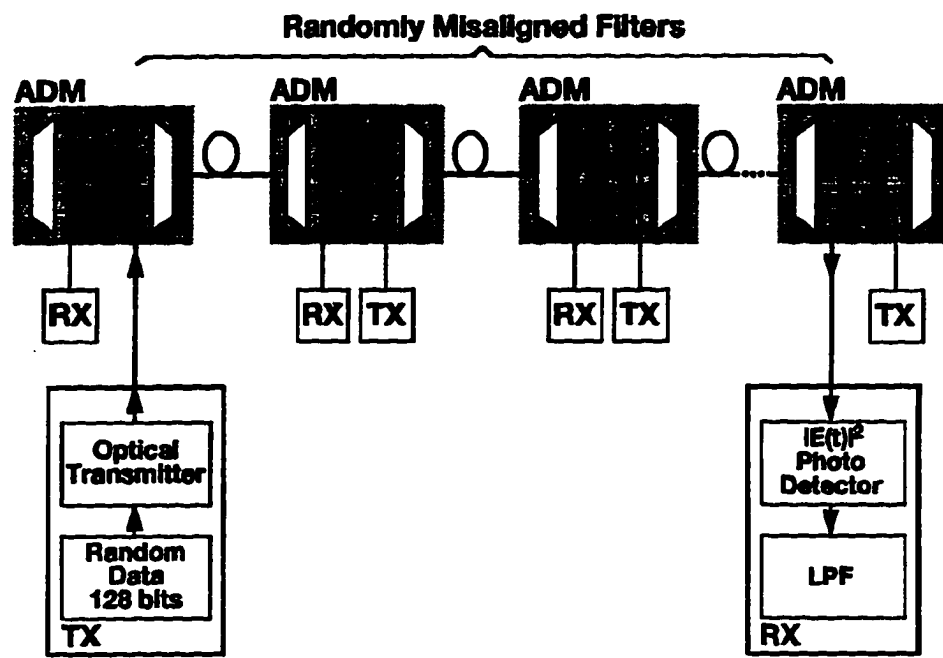
networks using first-order filters require more stringent control of misalignments than multiwavelength optical networks using third-order filters. Laser misalignment of ± 20 GHz produces 14 dB system excess loss and 0.3 dB distortion-induced eye-closure penalty if first-order Butterworth filters are used.

Table 3.2 summarizes the required misalignment tolerances for the three criterion used: 1 dB system excess loss, 0.3 dB distortion-induced penalty and at 1 dB distortion-induced penalty.

3.4 Conclusion

Computer simulation techniques have been used to evaluate the limitations on laser misalignment tolerances for WDM networks with a cascade of 30 (de)multiplexers modeled as either third-order or first-order Butterworth filters. The (de)multiplexers are assumed to be uniformly misaligned over a range up to ± 12.5 GHz. The results are significantly dependent on the type of filter used, and do not depend strongly on the modulation speed and technique. Multiwavelength optical networks using (de)multiplexers modeled as third-order Butterworth filters require less stringent control of laser misalignment compared to networks using (de)multiplexers modeled as first-order Butterworth filters. Distortion induced eye-closure penalty may not be easily overcome in multiwavelength optical networks but the excess loss can be overcome by the gain provided by optical amplifier cascades. For WDM systems with 30 uniformly misaligned filters, laser misalignment tolerances at 0.3 dB distortion-induced eye-closure penalty vary

from ± 30 GHz (± 0.24 nm) for systems using third-order filters to ± 20 GHz (± 0.16 nm) for systems using first-order filters.



ADM = Add & Drop Multiplexer

Figure 3.1: Simulation block diagram for a lightwave system with a cascade of randomly misaligned multiplexers and demultiplexers.

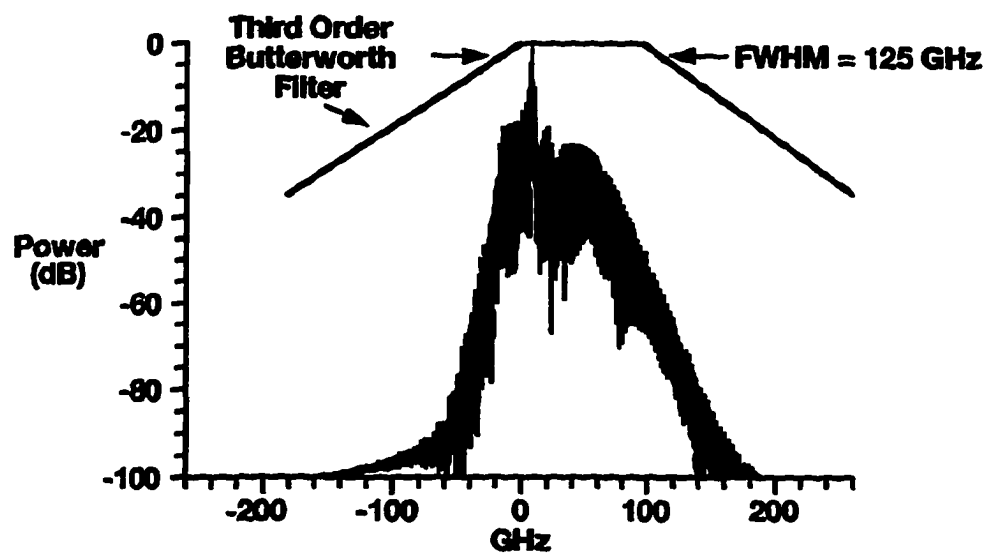


Figure 3.2: Time average spectrum of a MQW-DFB laser directly modulated at 2.5 Gb/s. The transmittance characteristic of a third-order Butterworth filter is also shown.

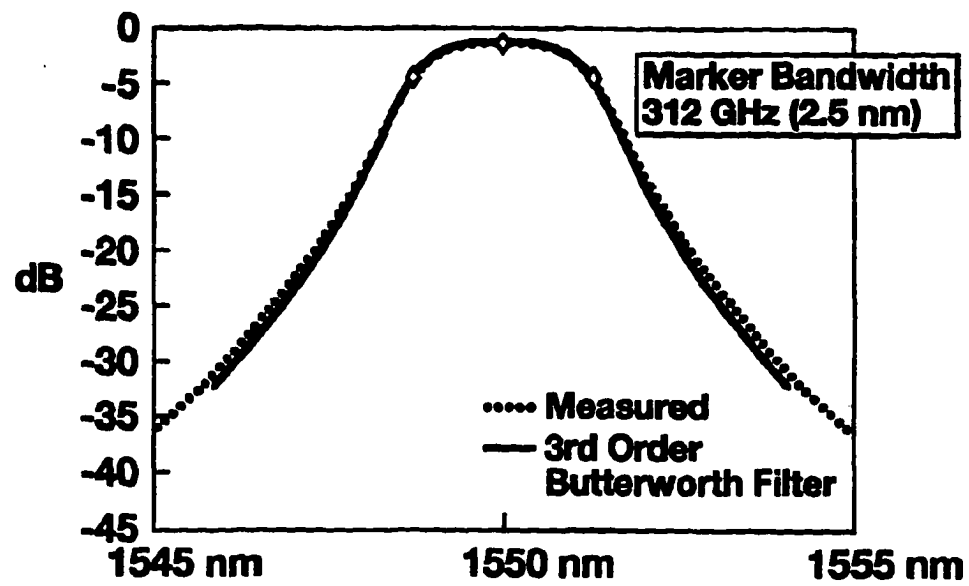


Figure 3.3: The transmittance characteristic of a multi-layer dielectric film optical (de)multiplexer.

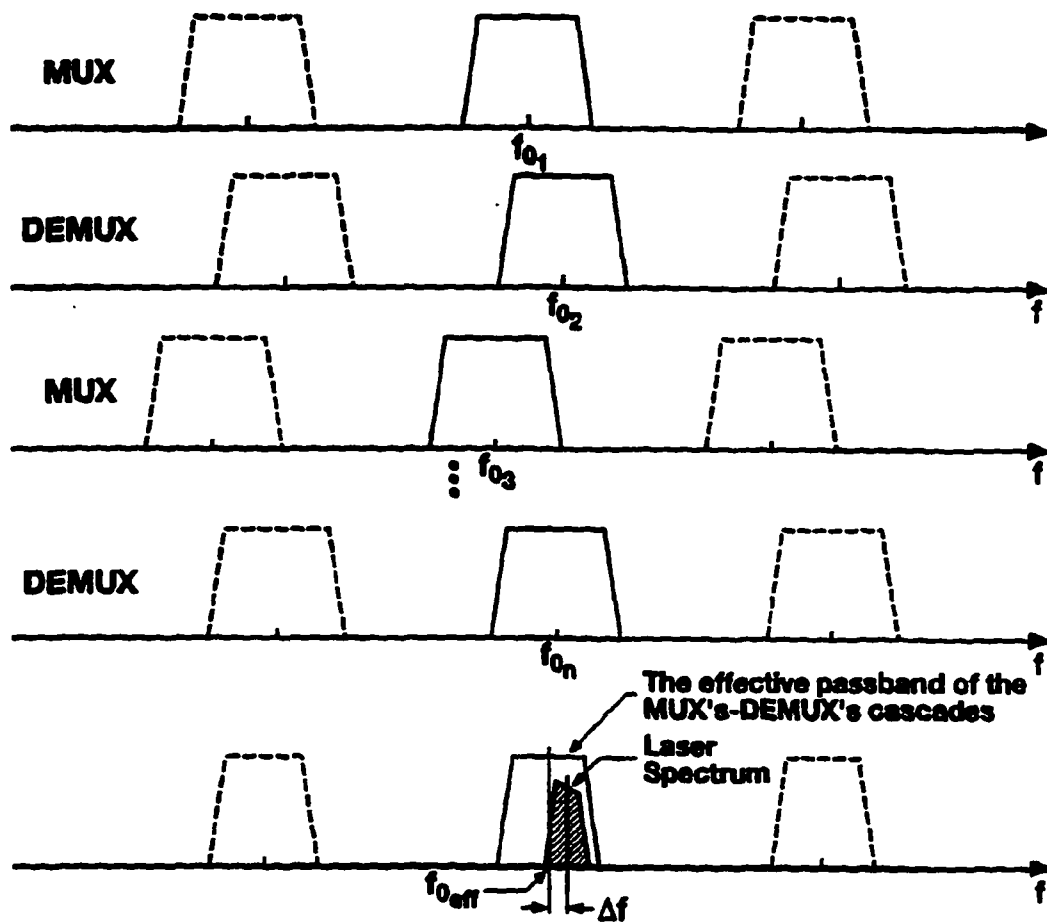


Figure 3.4: Laser spectrum misalignment relative to the center frequency of the effective passband of the uniformly distributed concatenated multiplexers and demultiplexers.

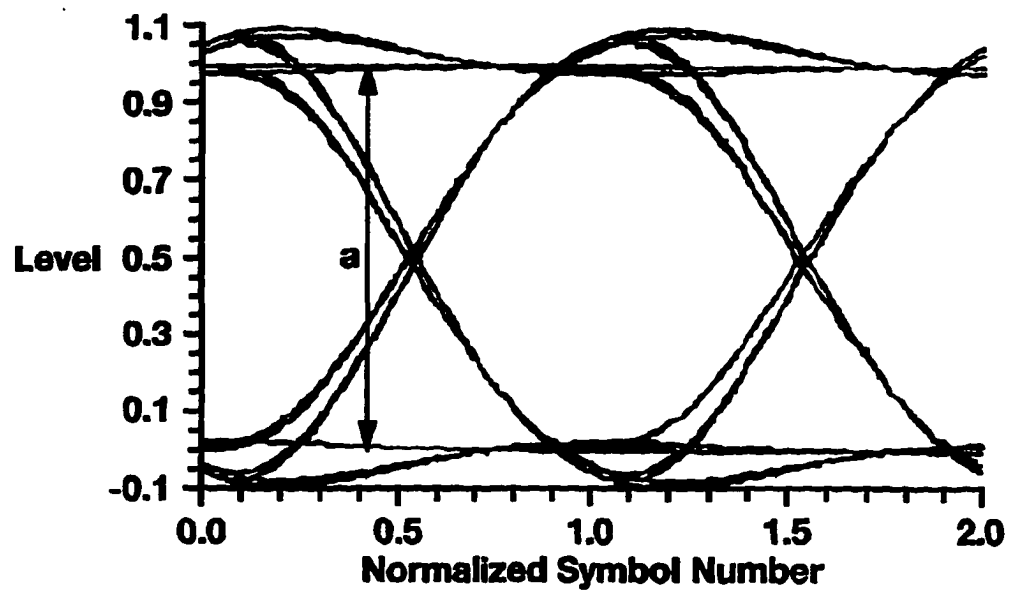


Figure 3.5a: Received eye-diagram at 10 Gb/s for lightwave systems with no optical filters.

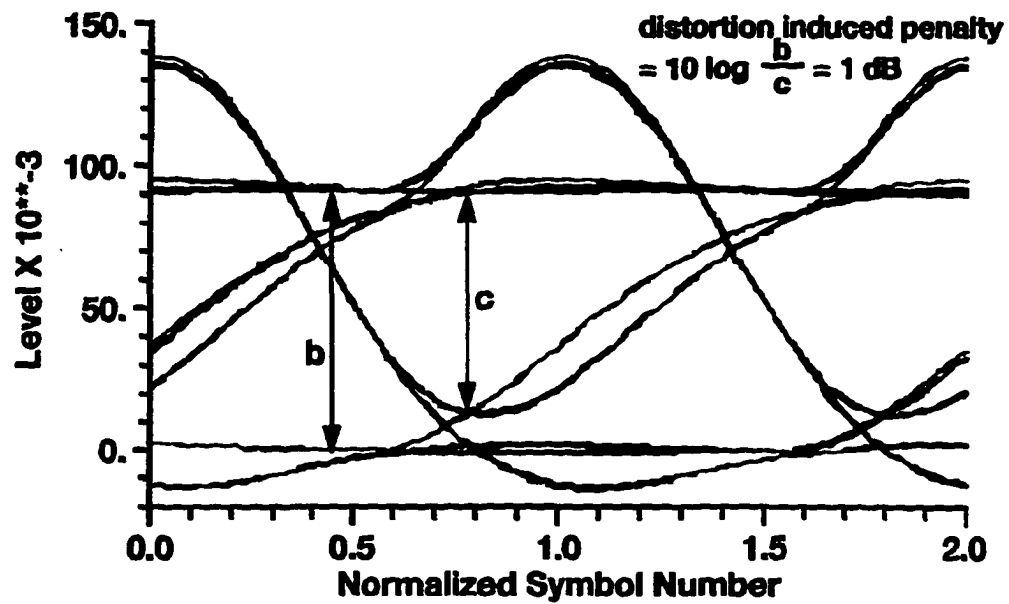


Figure 3.5b: Received eye-diagram at 10 Gb/s for lightwave systems with 30 uniformly distributed (de)multiplexers modeled as third-order Butterworth filters and ± 38 GHz laser misalignment.

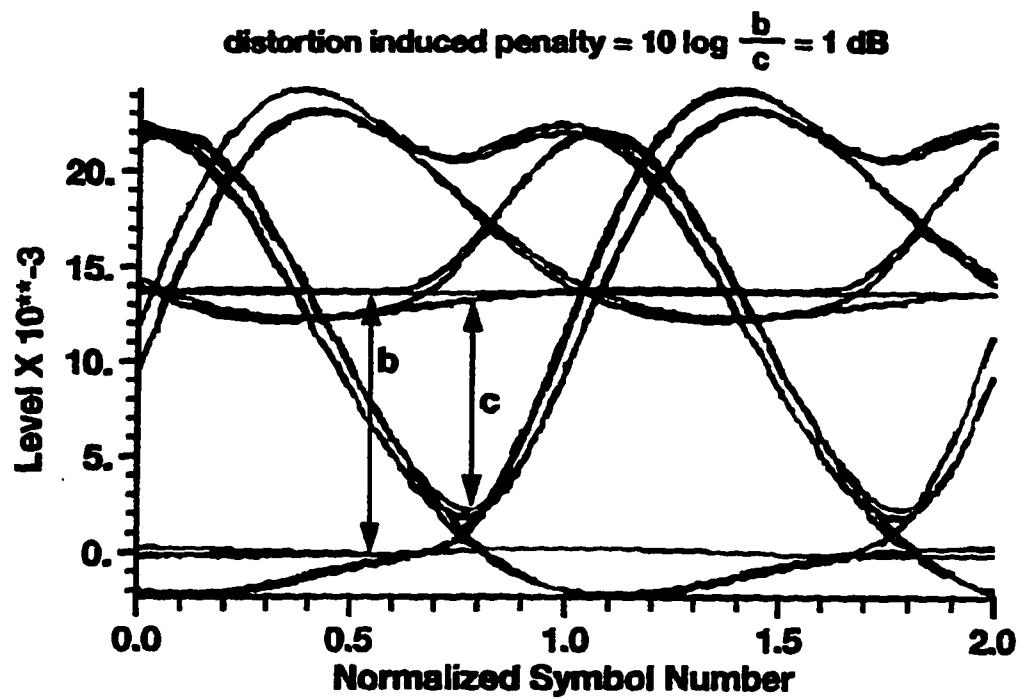


Figure 3.5c: Received eye-diagram at 10 Gb/s for lightwave systems with 30 uniformly distributed (de)multiplexers modeled as first-order Butterworth filters and ± 24 GHz laser misalignment.

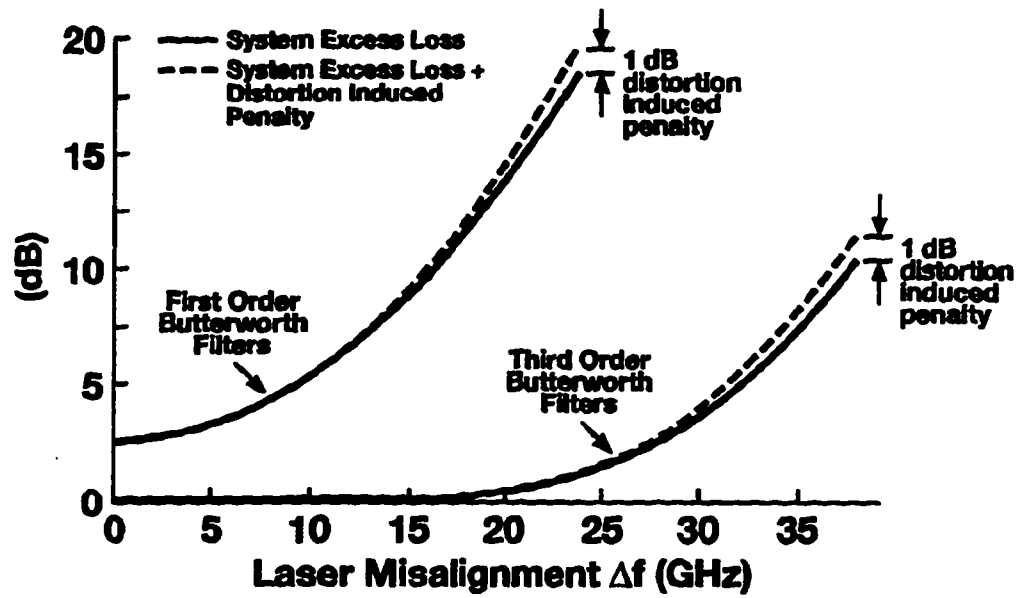


Figure 3.6a: System excess loss plus distortion-induced eye-closure penalty versus laser misalignment for a WDM network with 30 uniformly distributed (de)multiplexers.

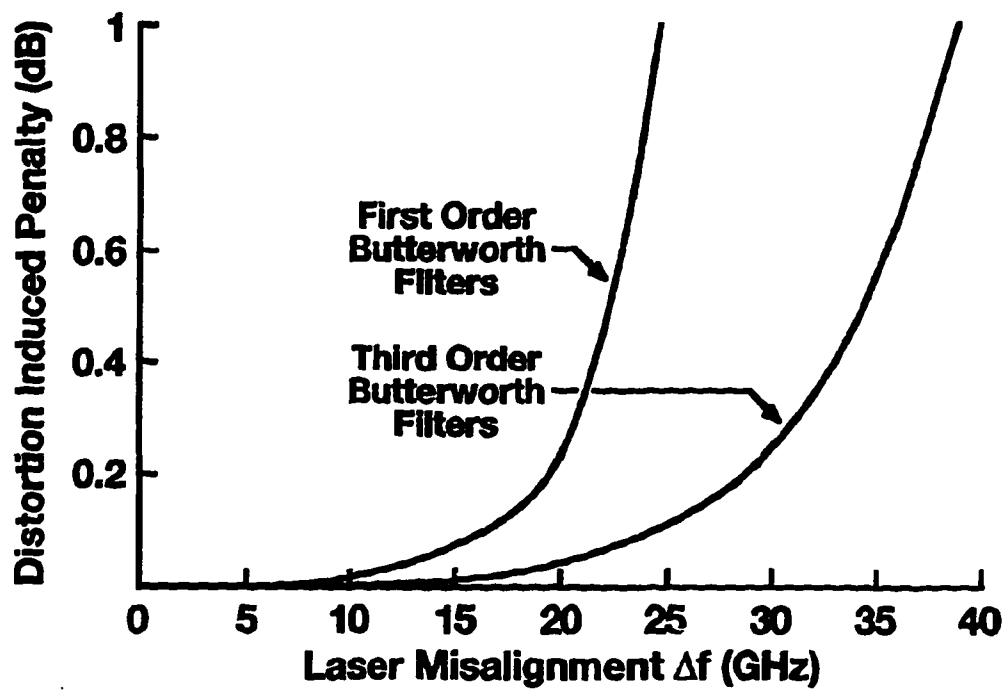


Figure 3.6b: Distortion-induced eye-closure penalty versus laser misalignment for a WDM network with 30 uniformly distributed (de)multiplexers.

Number of Filters	Centered at δf (GHz)
6	-12.5
6	-6.25
6	0
6	6.25
6	12.5
Total = 30	Effective Center Frequency = 0

Table 3.1: Misaligned (de)multiplexers distribution over a range of up to ± 12.5 GHz (± 0.1 nm).

Laser Misalignment Tolerances

Filter Alignment Filter Type	Perfectly Aligned			Uniformly Misaligned		
	1 dB Sys. Excess Loss	0.3 dB Distortion Induced Penalty	1 dB Distortion Induced Penalty	1 dB Sys. Excess Loss	0.3 dB Distortion Induced Penalty	1 dB Distortion Induced Penalty
First Order	±6 GHz	±20 GHz	±24 GHz	*	±20 GHz	±24 GHz
Third Order	±29 GHz	±30 GHz	±38 GHz	±23 GHz	±30 GHz	±38 GHz

*System excess loss is higher than 1 dB.

Table 3.2: Laser misalignment tolerances for WDM systems at 2.5 Gb/s or 10 Gb/s per optical channel with 30 (de)multiplexers modeled as either third-order or first-order Butterworth filters.

Chapter 4

Performance of Cascaded Misaligned Optical (De)multiplexers in Multiwavelength Optical Networks for 2-100 (de)multiplexers in Cascade

4.1 Introduction

Multiwavelength optical networks, using wavelength selective components, are recognized as an attractive technology option for building a flexible optical network layer [6], [7], [18]. It is becoming clear that such network architectures may cause degradation of the optical signal, chiefly because of the combined effects of the concatenation and the misalignment of the (de)multiplexers [25], [26]. Degradation may also be due to the fact that laser array technology provides less control of the laser wavelengths, relative to the effective center frequency of the (de)multiplexer cascades, than discrete single-channel devices [24].

A typical multiwavelength optical network consists of a number of network elements (see Fig. 4.1), which may drop and add individual wavelengths via (de)multiplexer components. The optical signal passes through many network elements, and hence many (de)multiplexers, before it reaches its destination at

the receiver. In this paper we use computer simulation techniques to evaluate the effect of laser misalignment tolerances on a multiwavelength optical network for various number of network elements in a cascade. The number of network elements considered varies between one network element (2 (de)multiplexers) and 50 network elements (100 (de)multiplexers). The (de)multiplexers considered in this study are assumed to be either perfectly aligned or randomly misaligned. For lightwave systems using wavelength division multiplexing (WDM) technology with 200 GHz or more channel spacing, crosstalk is small enough to be neglected in this study.

4.2 The System Model

The simulation block diagram for the WDM system considered is shown in Fig. 4.1. The system consists of a transmitter externally modulated either at 2.5 Gb/s or 10 Gb/s per optical channel, a cascade of randomly misaligned optical (de)multiplexers as part of a network element cascade, and a receiver. The electric field at the output of the laser facet (input to the network element cascade) is expressed by:

$$E_{in}(t) = \sqrt{P_{ext}(t)}, \quad (4.1)$$

where P_{ext} is the output power from the external modulator, simulated as an NRZ random data sequence of length equal to 128 bits.

The two types of (de)multiplexers considered in the simulation are modeled as

first-order and third-order Butterworth filters, each with a FWHM of 125 GHz (1 nm) and a filter center frequency misalignment of δf . The theoretical filter shape used in the simulation represents WDM Fabry-Perot [6] filter (de)multiplexers for first-order, and dielectric-film (de)multiplexers for third-order. A comparison of measured and theoretical filter shapes is shown in Fig. 4.2 for third order Butterworth filters [3, 4].

The electric field at the output of the cascade (input to the receiver) is expressed by:

$$E_{\text{out}}(t) = \sqrt{P_{\text{ext}}}(t) * F^{-1} \left\{ \prod_{i=1}^n H(f - f_o - \delta f_i) \right\}, \quad (4.2)$$

where $|H(\cdot)|^2$ is the transmittance characteristic of each optical filter, f is the optical frequency, f_o is the center frequency of each optical filter, and the number (n) of (de)multiplexer in the cascade varies between 2 and 100. The receiver electrical filter is modeled as a third-order Butterworth filter with a 3 dB bandwidth equal to 0.65 times the bit rate in order to minimize the receiver noise while maximizing the eye opening.

Two cases are considered in the simulation. In the first case, the center frequencies of all cascaded (de)multiplexers are assumed to be perfectly aligned. In the second case, the center frequency misalignment (δf) of the individual (de)multiplexers is assumed to be randomly misaligned with a uniform distribution of frequency offsets, within the range of ± 12.5 GHz (± 0.1 nm). The laser misalignment (Δf) is defined as the difference between the center frequency

of the laser spectrum under modulation and the center frequency of the effective passband of the concatenated (de)multiplexers. If the laser misalignment becomes large, the optical signal is distorted as it passes through the side of the filter passband, causing eye closure. Allowable laser misalignment (Δf) versus number of (de)multiplexers is calculated at 0.3 dB distortion-induced eye-closure penalty, for the system under study relative to the case without (de)multiplexers. The distortion-induced eye-closure penalty for the WDM system under study is given by $10 \log(a / b)$, where (a) is the signal level difference between logical ONE and ZERO calculated for the WDM system under study, and (b) is the eye opening for the WDM system under study as shown in Fig. 4.3. This definition does not include the penalty due to transmission loss of the filters, which can be compensated by gain in the network elements.

4.3 Simulation Results

Fig. 4.4 shows laser misalignment tolerances versus number of (de)multiplexers in a cascade, assuming external modulation at 10 Gb/s per optical channel. Laser misalignment tolerances are approximately the same using either perfectly aligned or randomly misaligned (de)multiplexers modeled as third order Butterworth filters. This is due to the combined effects of the symmetrical distribution of the misalignment, the assumed small range of misalignment compared to the FWHM of the (de)multiplexers, and the fact that the spectral width of the optical signal at 10 Gb/s is larger than the difference between the effective passbands of

the perfectly aligned and randomly misaligned (de)multiplexers.

Fig. 4.4 also shows that WDM systems with a cascade of up to 10 perfectly aligned (de)multiplexers modeled as first-order filters have larger laser misalignment tolerances than systems using (de)multiplexers modeled as third-order filters. This is because the tail decay of the first-order filters is relatively slow, and is a dominant factor of determining the tolerances, compared to the tail decay of the effective transmittance characteristic of a cascade of (de)multiplexers modeled as third-order filters (e.g. see Fig. 4.5a). This gives the optical signal spectrum a degree of freedom to drift from the center frequency of the effective passband of the (de)multiplexers, while retaining a large amount of the signal energy inside the effective channel.

The situation is different when more than 10 perfectly aligned (de)multiplexers are cascaded (see Fig. 4.4). Now the third-order Butterworth filters allow a larger laser misalignment tolerance than systems using first-order filters. This is because the tail decay of the effective transmittance characteristic of a cascade of a large number of (de)multiplexers modeled as first-order filters becomes almost as steep as the third-order filter cascade (e.g. see Fig. 4.5b). At the same time the flat top region becomes smaller for first-order filters cascades, causing them to have more stringent misalignment tolerances than systems using (de)multiplexers modeled as third-order Butterworth filters.

For the randomly aligned case, the assumed misalignment of ± 12.5 GHz for (de)multiplexers modeled as first-order filters causes an even narrower effective passband than the perfectly aligned case, which leads to even more severe limitations on the laser misalignment tolerances. A cascade of more than 60 (de)multiplexers modeled as first-order filters becomes impossible without unacceptably large system penalties, as shown in Fig. 4.4.

Multiwavelength optical networks operating at 2.5 Gb/s have more relaxed laser misalignment tolerances than systems operating at 10 Gb/s as shown in Fig. 4.6. This is due to the fact that the spectral width of the optical signal at 2.5 Gb/s is narrower than the spectral width of the optical signal at 10 Gb/s.

4.4 Conclusions

Computer simulation techniques have been used to evaluate laser misalignment tolerances of a multiwavelength optical network at 0.3 dB distortion-induced eye-closure penalty, for a network with 1 to 50 network elements in cascade. The (de)multiplexers considered are modeled as third-order Butterworth filters and first-order filters and assumed to be either perfectly aligned or randomly misaligned with uniform distribution over ± 12.5 GHz. The results are dependent on the number of (de)multiplexers used, on the bit rate and on the filter shape.

For multiwavelength optical networks at 10 Gb/s with randomly misaligned (de)multiplexers modeled as third-order Butterworth filters, laser misalignment tolerances vary from ± 78 GHz (± 0.63 nm) for systems with 1 network element to ± 18 GHz (± 0.15 nm) for systems with a cascade of 50 network elements.

However, for systems at 10 Gb/s with randomly misaligned (de)multiplexers modeled as first-order filters, laser misalignment tolerances vary from ± 180 GHz (± 1.44 nm) with 1 network element to ± 5 GHz (± 0.04 nm) with a cascade of 30 network elements. With first-order filters a cascade of 50 network element is not possible without unacceptably large system penalties.

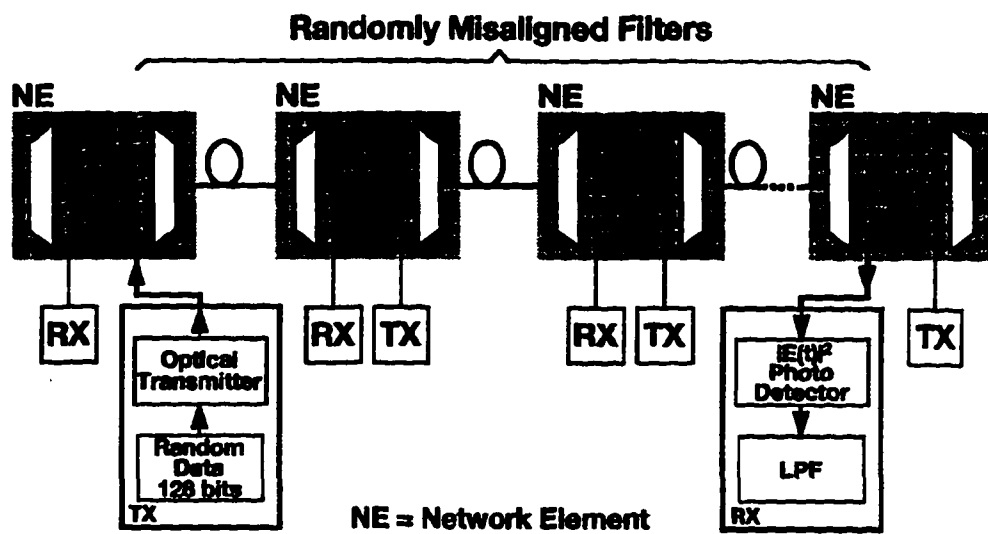


Figure 4.1: Simulation block diagram for a lightwave system with a cascade of randomly misaligned multiplexers and demultiplexers.

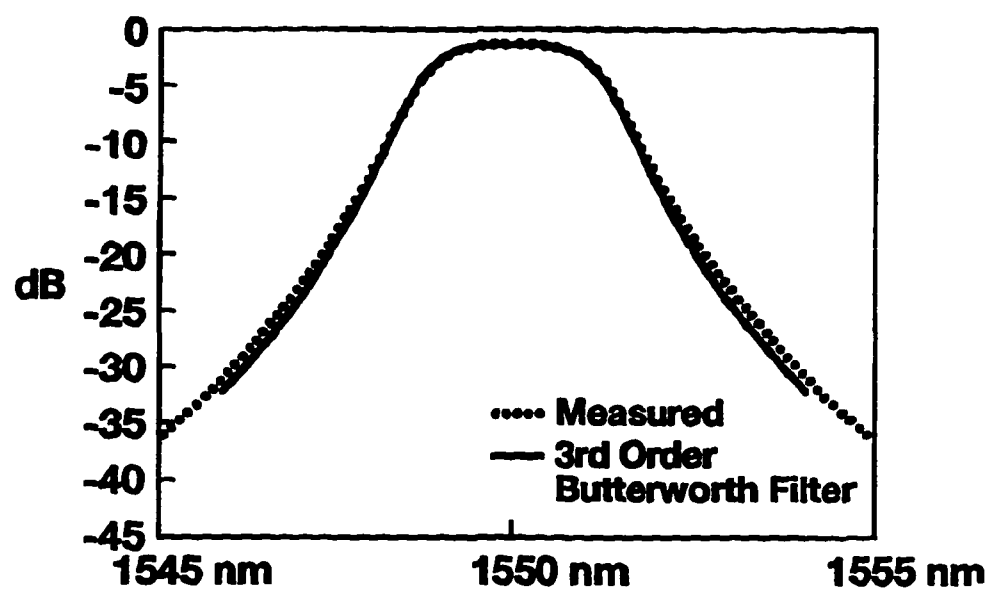


Figure 4.2: The transmittance characteristic of a multi-layer dielectric film optical (de)multiplexer.

$$\text{distortion-induced penalty} = 10 \log \frac{a}{b} = 0.3 \text{ dB}$$

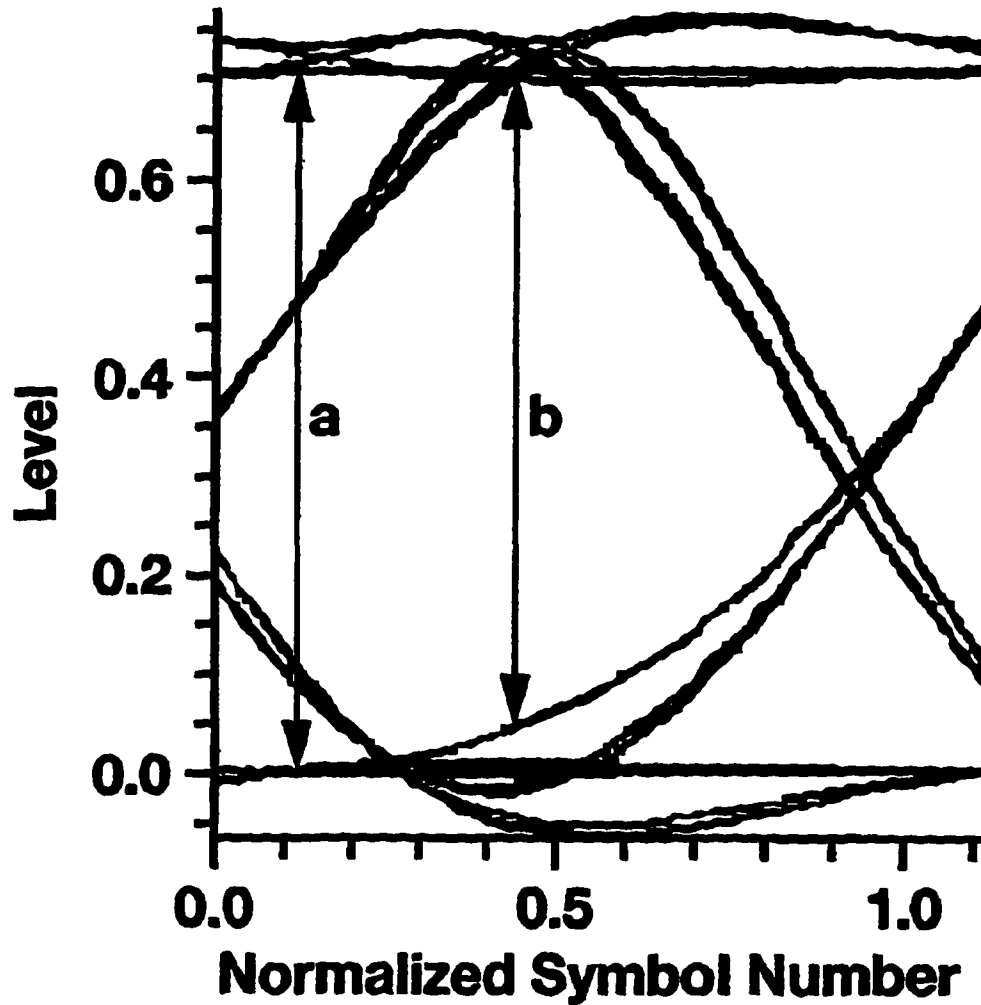


Figure 4.3: Received eye-diagram at 0.3 dB distortion-induced eye-closure penalty for lightwave systems modulated at 10 Gb/s with 100 randomly misaligned (de)multiplexers modeled as third-order Butterworth filters and ± 18 GHz laser misalignment.

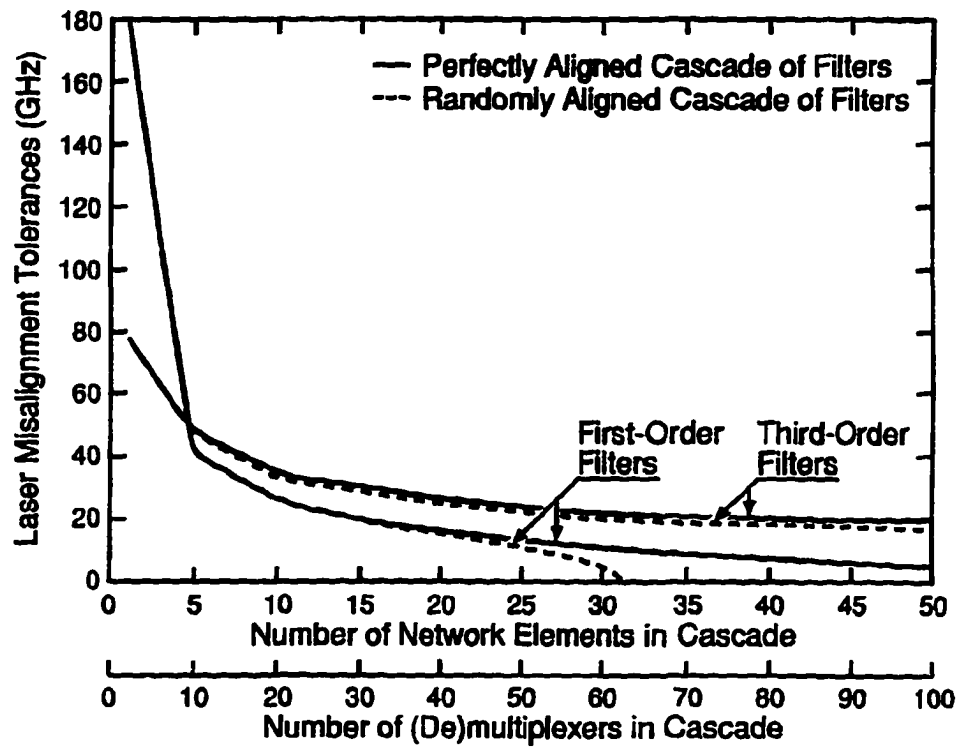


Figure 4.4: Laser misalignment tolerances versus number of perfectly aligned and randomly misaligned (de)multiplexer cascades for a WDM optical network operating at 10 Gb/s per optical channel.

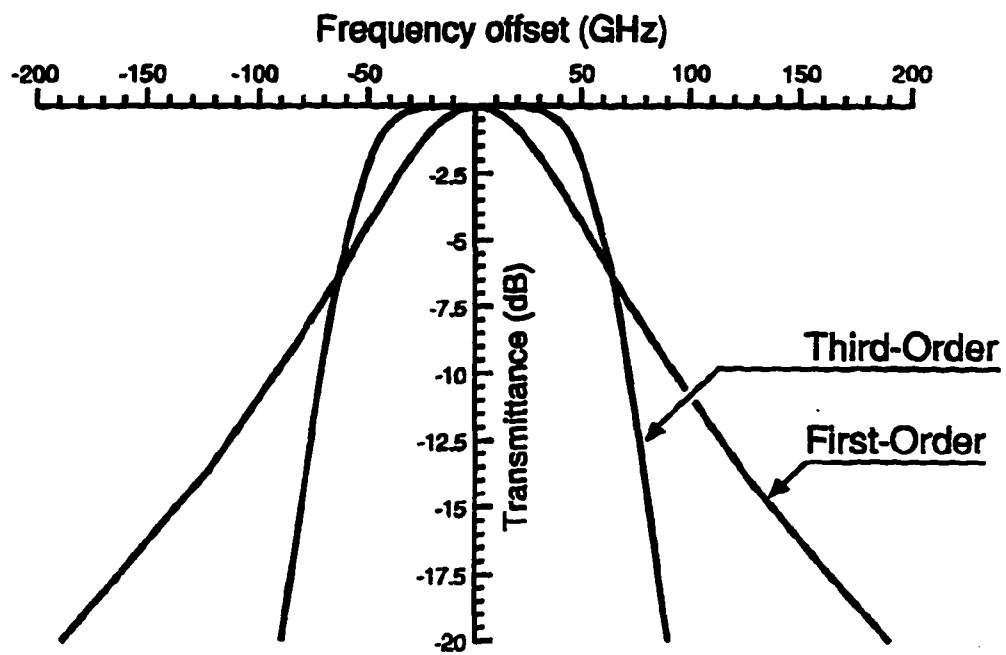


Figure 4.5a: The effective transmittance characteristic of perfectly aligned 2 (de)multiplexers in cascade (1 network element).

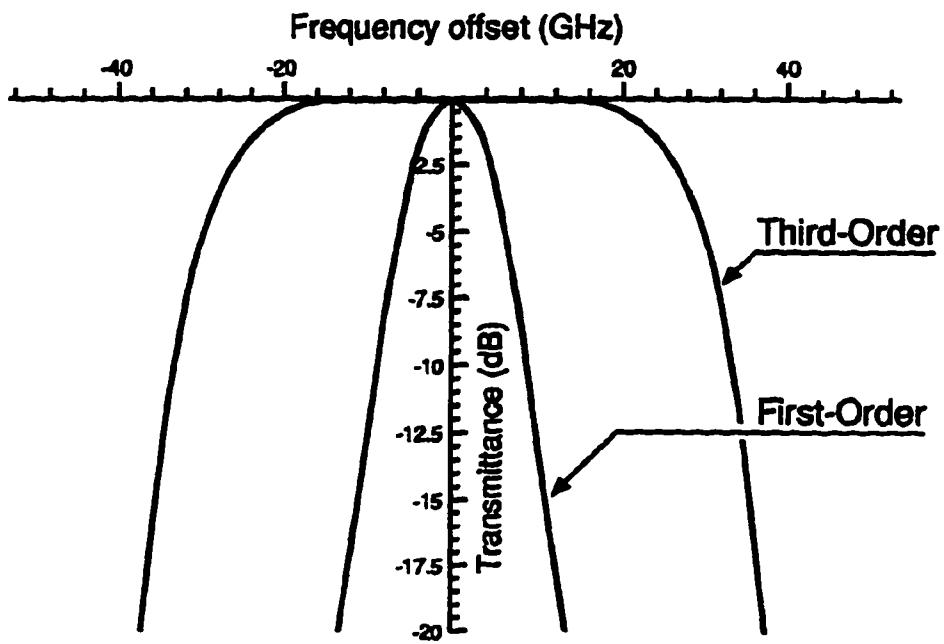


Figure 4.5b: The effective transmittance characteristic of perfectly aligned 100 (de)multiplexers in cascade (50 network elements).

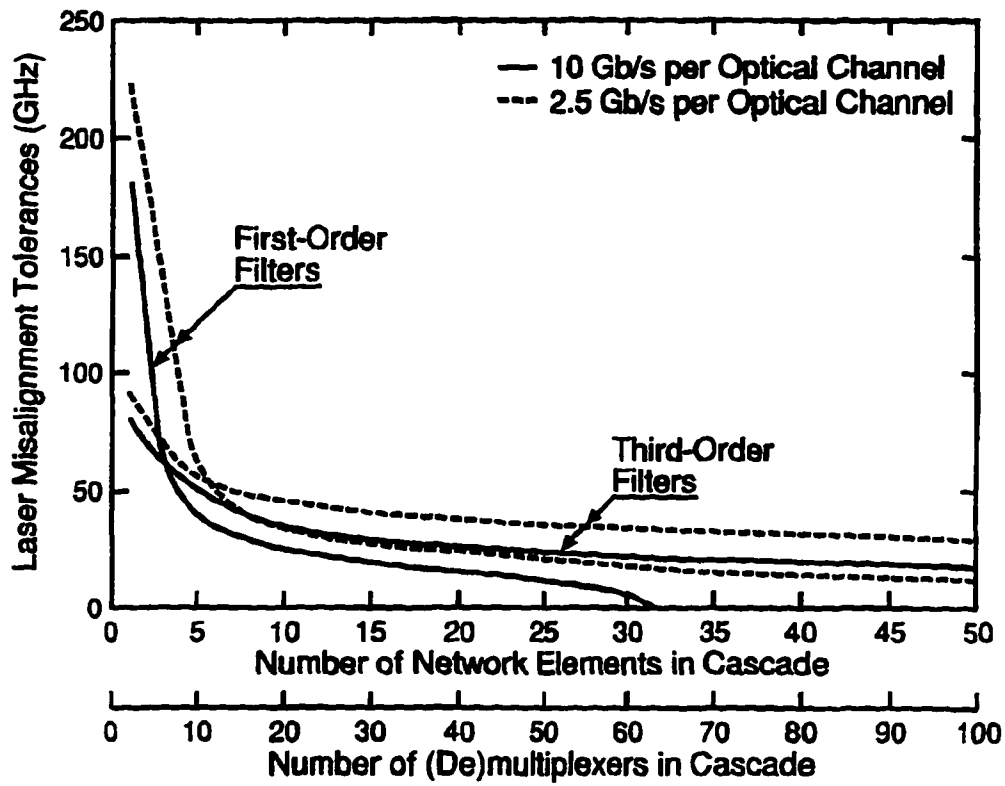


Figure 4.6: Laser misalignment tolerances versus number of randomly misaligned (de)multiplexers in cascade for a WDM optical network operating at either 2.5 Gb/s or 10 Gb/s per optical channel.

Chapter 5

Multiplexer Eye-Closure Penalties for 10 Gb/s Signals in WDM Networks: Simulation Versus Experiment

5.1 Introduction

Multiwavelength optical networks using wavelength selective components are recognized as an attractive technology option for building a flexible optical network layer [6], [7], [18]. It is becoming clear that such network architectures may cause degradation of the optical signal due to the combined effects of the multiplexer and demultiplexer concatenation together with the misalignment of the (de)multiplexers and the laser source optical frequency [25], [26].

An optical (de)multiplexer can be represented mathematically by its transfer function, which consists of a magnitude component and a phase component. In this paper, we use computer simulation techniques to determine the distortion-induced penalty versus laser misalignment for an optical network with a cascade of 8 multiplexers and 8 demultiplexers. The penalty has a contribution due to the frequency-dependent magnitude of the transfer function and a contribution due to the phase of the transfer function as well. The simulation results are supported by experimental measurements of transmission performance through a cascade of 6 pairs of phased-array multiplexers and demultiplexers, and 2 pairs of

multi-layer dielectric film multiplexers and demultiplexers.

5.2 (De)Multiplexer Model

The transfer function of the multiplexers and demultiplexers is assumed to have the shape of a third-order Butterworth filter, including both magnitude and phase characteristics. Figure 5.1 shows a comparison of the magnitude of the theoretical filter shape and an experimentally measured filter shape of one of the phased array multiplexers, indicating that the overall shape and roll off is well represented by the Butterworth filter.

In general, the transfer function $H(f)$ of each (de)multiplexer is represented by:

$$H(f) = M(f)e^{j\theta(f)}, \quad (5.1)$$

where $M(f)$ is the magnitude and $\theta(f)$ is the phase of the transfer function. The magnitude of the transfer function $M(f)$ can be expanded about the laser center frequency f_0 :

$$M(f) = M(f_0) + \frac{d}{df}M(f)|_{f_0} (f - f_0) + \frac{1}{2!} \frac{d^2}{df^2}M(f)|_{f_0} (f - f_0)^2 + \dots \quad (5.2)$$

The first term in the expansion is a constant which represents the loss of the filter; it is compensated by amplifier gain in other parts of the network and introduces no system penalty. The second and the third terms are found to be sufficient for approximating the contribution of the magnitude to the distortion-induced penalty.

Similarly, the phase portion of the transfer function $\theta(f)$ can also be expanded as:

$$\theta(f) = \theta(f_0) + \frac{d}{df}\theta(f)|_{f_0} (f - f_0) + \frac{1}{2!} \frac{d^2}{df^2}\theta(f)|_{f_0} (f - f_0)^2 + \dots \quad (5.3)$$

In the above expansion, the first term is the phase offset and the second term represents a fixed delay, neither of which contribute to distortion-induced system penalties. The third term is a dispersion-like effect which contributes to the distortion-induced penalty. It is found to be sufficient for approximating the phase contribution to the distortion.

5.3 Simulation and Experimental Results

The simulation consists of finding an equivalent transfer characteristic that is the product of each of the 8 multiplexer and 8 demultiplexer transfer functions. The measured bandwidths and center frequency offsets of each of the (de)multiplexers were used in the simulation assuming third order Butterworth filter shapes for each. The frequency offsets ranged between 0 and 21 GHz, and the 3-dB bandwidths ranged from 121 to 145 GHz as given in Table 5.1. A perfect external modulation at 10 Gb/s, without chirp, was applied to the simulated laser source and a simulation eye pattern was computed. The distortion-induced eye-closure penalty was calculated at a variety of laser frequency misalignments from the center of the equivalent transfer characteristic. The range of laser frequency misalignments was from -50 to +50 GHz. The method of calculation is described in detail in Reference [25].

Figure 5.2 shows the received eye diagrams at laser frequency misalignments of 12.3 GHz where the system penalty is small, and also at 37 GHz (experiment) and 42 GHz (simulation) where the system penalty is about 0.5 dB. The eye patterns indicate that the results of the simulation and the experiment are similar.

The resulting distortion-induced penalty is plotted versus laser frequency misalignment in Figure 5.3. The lower curve (shown solid) represents the penalty introduced by the magnitude of the transfer characteristic only; the middle curve (shown dotted) represents the penalty due to both phase and magnitude of the transfer characteristic. The upper curve (shown with asterisks) indicates the experimentally measured penalty as a function of laser frequency misalignment. The experimental curve is very similar to the simulation results, except that it has slightly more penalty at each misalignment. This difference could be due to a variety of causes, including the inaccuracy of the fit of the magnitude of the transfer function, the fact that the external modulation used for the experiment is accompanied by a little chirp, and the possibility that the phase of the transfer function of the real filters produces more penalty than the assumed phase of the Butterworth filters.

5.4 Summary

These results make two important points. First, simulation techniques can be used to estimate the laser misalignment tolerances for cascades of multiplexers and demultiplexers fairly well. Second, the phase characteristics of (de)multiplexer transfer functions can be important in cascades, since they introduce dispersion-like system penalties. As a result, the phase characteristics of WDM multiplexers and demultiplexers should be measured to determine their suitability if they are to be used in network applications where cascades of multiplexers and demultiplexers occur.

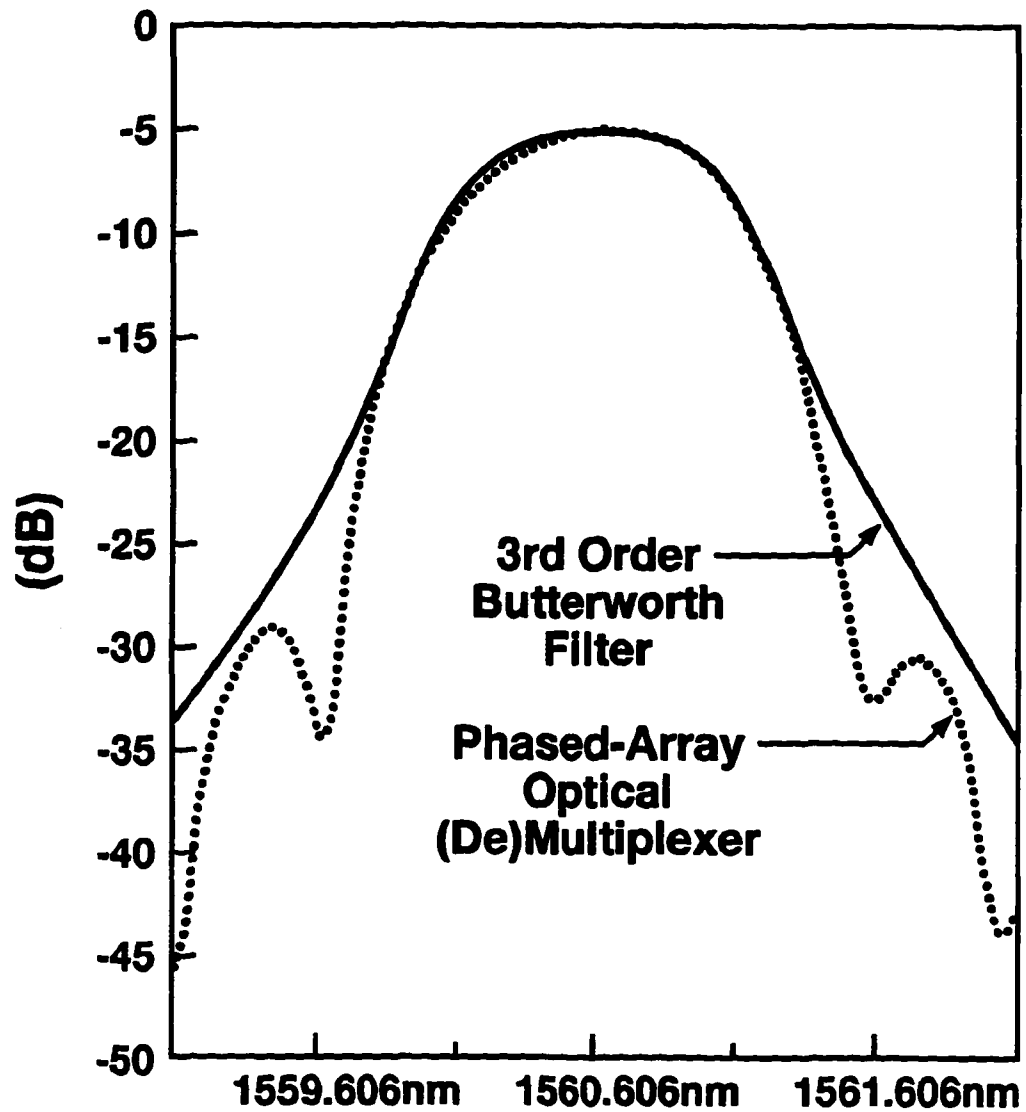


Figure 5.1: Comparison of theoretical and experimental multiplexer magnitude of the transfer function of a phased-array optical (de)multiplexer.

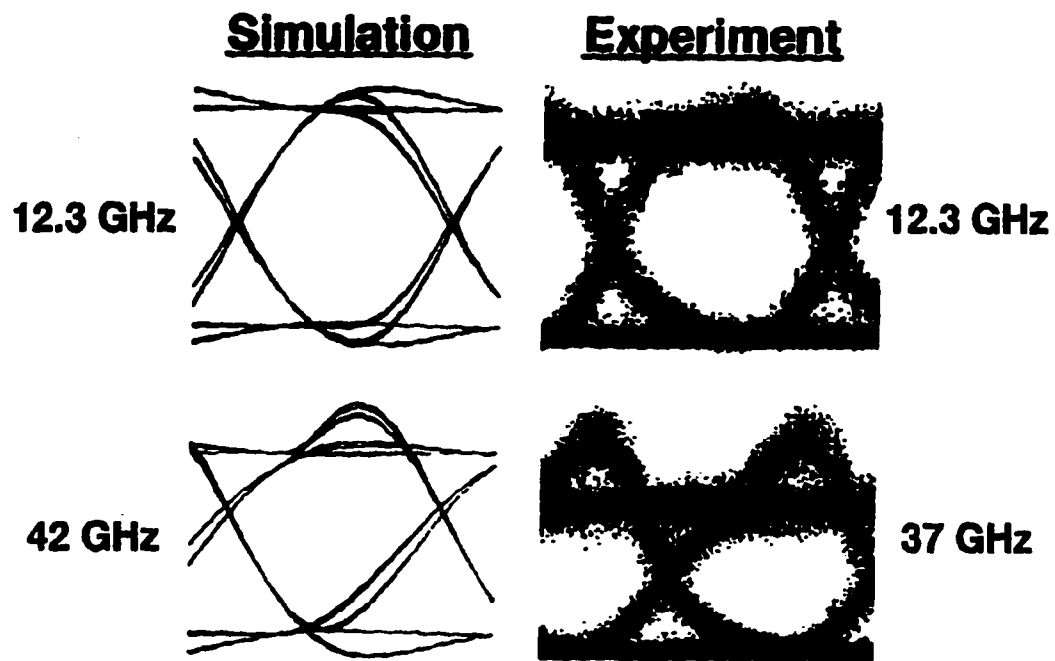


Figure 5.2: Received eye-diagrams at 10 Gb/s per optical channel for a WDM optical network with a cascade of 8 multiplexers and 8 demultiplexers.

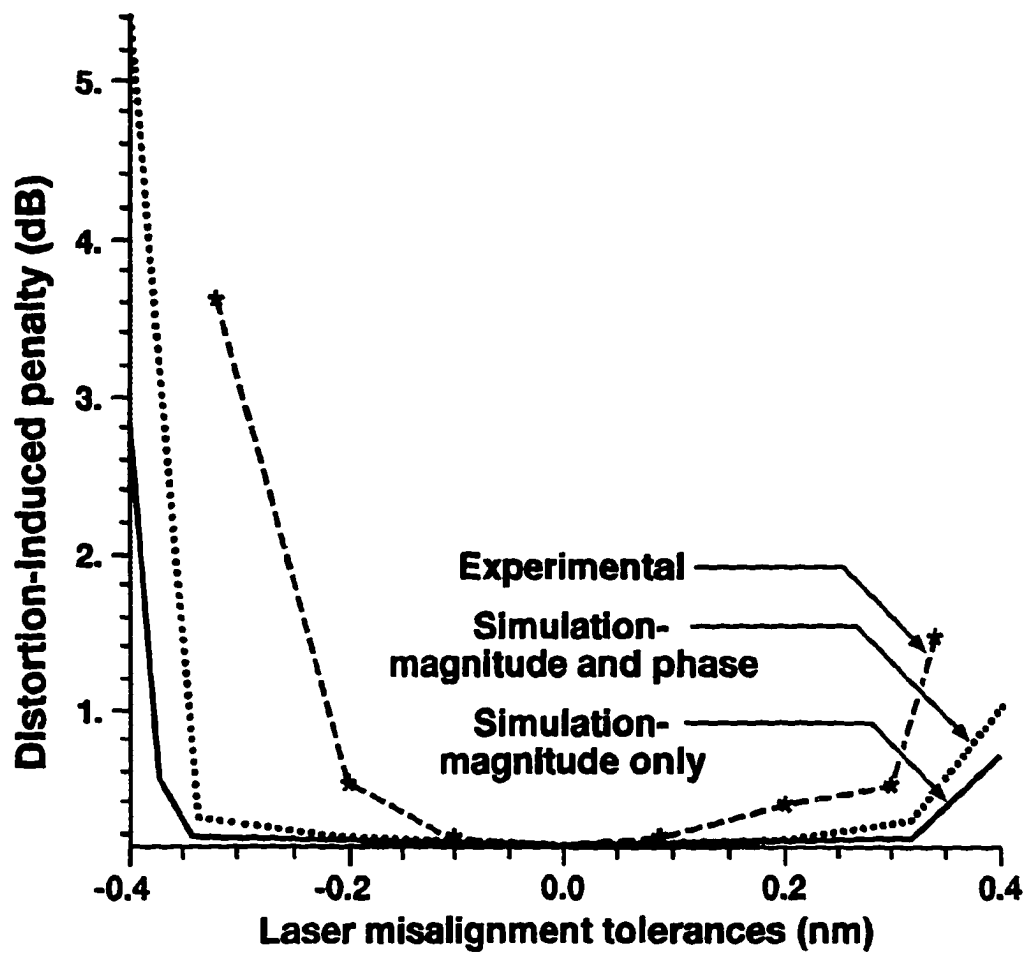


Figure 5.3: Distortion-induced eye-closure penalty versus laser frequency misalignment for a WDM optical network operating at 10 Gb/s per optical channel with a cascade of 8 multiplexers and 8 demultiplexers.

Phase-Array

#	3 dB - B.W.	Freq. Offset	#	3 dB - B.W.	Freq. Offset
1	123 GHz	2 GHz	2	122 GHz	21 GHz
3	123 GHz	12 GHz	4	121 GHz	0 GHz
5	122 GHz	0 GHz	6	123 GHz	0 GHz
7	123 GHz	0 GHz	8	124 GHz	0 GHz
9	123 GHz	0 GHz	10	121 GHz	0 GHz
11	122 GHz	0 GHz	12	122 GHz	0 GHz

Multi-Layer

13	142 GHz	0 GHz	14	137 GHz	0 GHz
15	145 GHz	0 GHz	16	137 GHz	0 GHz

Table 5.1: Optical multiplexer and demultiplexer characteristics.

Chapter 6

General (De)multiplexer Cascade Model for Transparent Digital Transmission

6.1 Introduction

Multiwavelength optical networks using wavelength selective components are recognized as an attractive technology option for building a flexible optical network layer [27, 28]. It is becoming clear that such network architectures may cause degradation of the optical signal due to the combined effects of the multiplexer and demultiplexer concatenation together with the misalignment of the (de)multiplexers and the laser source optical frequency [25]. Degradation due to both the magnitude and the phase characteristics of the (de)multiplexers are important [29]

Previous work has been done to find the acceptable laser frequency misalignment tolerances in multiwavelength optical networks [25, 30]. The limitation in that work is that to compute the allowable laser misalignment tolerances for a specific situation, the number of (de)multiplexers in cascade, the (de)multiplexer filter shape and filter phase, the 3-dB bandwidth, and the bit rate all must be known.

This work overcomes that limitation by defining an equivalent transfer function for the cascade, and then generating engineering rules for system penalties of the equivalent filter. This produces a (de)multiplexer cascade model that is general for any bit rate, any filter shape and phase, and any bandwidth. This model is also general for any number of (de)multiplexers in a cascade, since the magnitude of the equivalent filter is equal to the product of all the magnitudes of the multiplexers in the cascade, and the phase is the sum of all the phases in the cascade.

6.2 (De)Multiplexer Model

For a multiwavelength optical network, the effective complex amplitude transfer function $H(f)$ of a cascade of (de)multiplexers is defined as:

$$H(f) = \prod_{i=1}^S H_i(f) \equiv e^{-\gamma(f)} = e^{-\alpha(f) - j\theta(f)}. \quad (6.1)$$

where $\alpha(f)$ is the absorption characteristic of the effective transfer function, $\theta(f)$ is the phase in radians, and S is the size of the network. Normally only the magnitude $|H(f)|^2$ of the transfer function is considered in evaluating system performance, but this does not take into account the phase characteristic $\theta(f)$. To be general, both $\alpha(f)$ and $\theta(f)$ must be considered.

The expansion of the absorption characteristic about the laser center frequency f_0 is given by:

$$\begin{aligned} \alpha(f) = & \alpha(f_0) + \left\{ \frac{d}{df} \alpha(f) \Big|_{f_0} \right\} (f - f_0) + \frac{1}{2!} \left\{ \frac{d^2}{df^2} \alpha(f) \Big|_{f_0} \right\} (f - f_0)^2 \\ & + \frac{1}{3!} \left(\frac{d^3}{df^3} \alpha(f) \Big|_{f_0} \right) (f - f_0)^3 + \dots \end{aligned} \quad (6.2)$$

The absorption characteristic of the (de)multiplexer cascade expressed in dB is given by: $k\alpha(f)$ where $k=10 \text{ Log}(e)=2.303$. In dB terms, the expansion can be rewritten as:

$$k\alpha(f) = m_0 + m_1 \left(\frac{f-f_0}{B}\right) + m_2 \left(\frac{f-f_0}{B}\right)^2 + m_3 \left(\frac{f-f_0}{B}\right)^3 + \dots \quad (6.3)$$

where: $m_0 = k\alpha(f_0)$

$$m_1 = k \frac{d}{df} \alpha(f)|_{f_0} B$$

$$m_2 = \frac{k}{2!} \frac{d^2}{df^2} \alpha(f)|_{f_0} B^2$$

$$m_3 = \frac{k}{3!} \frac{d^3}{df^3} \alpha(f)|_{f_0} B^3$$

The first term in the expansion (6.3) is a constant which represents the loss of the filter at the laser frequency f_0 ; it is compensated by amplifier gain in other parts of the network and introduces no system distortion-induced eye-closure penalty. The second and the third terms are found to be sufficient for approximating the contribution of the magnitude to the distortion-induced penalty. So we define the quantity $\Delta M(f)$ as

$$\Delta M(f) \equiv k\alpha(f) - m_0 \cong m_1 \left(\frac{f-f_0}{B}\right) + m_2 \left(\frac{f-f_0}{B}\right)^2, \quad (6.4)$$

where the coefficients m_1 and m_2 are in dB.

Similarly, the phase portion of the transfer function $\theta(f)$ can be expanded as:

$$\begin{aligned} \theta(f) = & \theta(f_0) + \left\{ \frac{d}{df} \theta(f) \Big|_{f_0} \right\} (f - f_0) + \frac{1}{2} \left\{ \frac{d^2}{df^2} \theta(f) \Big|_{f_0} \right\} (f - f_0)^2 \\ & + \frac{1}{3!} \left\{ \frac{d^3}{df^3} \theta(f) \Big|_{f_0} \right\} (f - f_0)^3 + \dots \end{aligned} \quad (6.5)$$

$$= \beta_0 + \beta_1 \left(\frac{f - f_0}{B} \right) + \beta_2 \left(\frac{f - f_0}{B} \right)^2 + \beta_3 \left(\frac{f - f_0}{B} \right)^3 + \dots, \quad (6.6)$$

where:

$$\beta_0 = \theta(f_0)$$

$$\beta_1 = B \frac{d}{df} \theta(f) \Big|_{f_0}$$

$$\beta_2 = \frac{1}{2!} B^2 \frac{d^2}{df^2} \theta(f) \Big|_{f_0}.$$

In expansion (6.6), the first term is the phase offset and the second term represents a fixed delay, neither of which contribute to distortion-induced system penalties. The third term is a dispersion-like effect which contributes to the distortion-induced penalty. It is found to be sufficient for approximating the phase contribution to the distortion. So we define the quantity $\Delta\theta(f)$ as

$$\Delta\theta(f) \equiv \theta(f) - \left\{ \beta_0 + \beta_1 \left(\frac{f - f_0}{B} \right) \right\} \cong \beta_2 \left(\frac{f - f_0}{B} \right)^2 \quad (6.7)$$

where the coefficient β_2 is in radians.

Equations (6.4) & (6.7) allow us to represent an equivalent filter by only these expansion terms, which introduce the same distortion as the transfer function of a cascade of (de)multiplexers in the network. The magnitude of the equivalent filter is represented by $\Delta M(f)$ and the phase is represented by $\Delta\theta(f)$.

6.3 System Model

The system penalties associated with $\Delta M(f)$ and $\Delta\theta(f)$ terms can be evaluated by computer simulation. Since the expansion terms are normalized by the bit rate B , the resulting penalties are applicable at any bit rate.

The simulation block diagram used in the computer analysis is shown in Fig. 6.1. The system consists of a transmitter externally modulated at B Gb/s per optical channel, the (de)multiplexer model, and a receiver. The receiver electrical filter is modeled as a third-order Butterworth filter with a 3 dB bandwidth equal to $0.65 B$ in order to minimize the receiver noise while maximizing the eye-opening. The electric field at the output of the laser facet (input to the equivalent filter) is expressed by:

$$E_{in}(t) = \sqrt{P_{ext}(t)}, \quad (6.8)$$

where P_{ext} is the output power from the external modulator, simulated as an NRZ data sequence with rectangular pulse shape and of length equal to 128 bits. The electric field at the output of the (de)multiplexer model (input to the receiver) is expressed by:

$$E_{out}(t) = \sqrt{P_{ext}(t)} * F^{-1}\{H(f)\}. \quad (6.9)$$

Two cases are considered in the simulation. In the first case, we study the system performance due to magnitude contribution to the distortion where

$H(f) = e^{-\{\Delta M(f)/k\}}$ and $\Delta\theta(f)$ is assumed to be zero. In the second case, we study

the system performance due to the phase contribution to the distortion where $H(f) = e^{-j\Delta\theta(f)}$ and $\Delta M(f)$ is assumed to be 0.

The laser misalignment f_0 is defined as the difference between the center frequency of the laser spectrum under modulation and the center frequency of the (de)multiplexer cascade. If the laser misalignment becomes large, the optical signal is distorted as it passes through the side of the filter passband where the magnitude of the transfer function varies with the frequency and the phase is not linear.

The magnitude characteristic of the equivalent filter is defined by the parameters m_1 and m_2 and the phase characteristic is defined by the parameter β_2 . We have found that the two parameters m_1 and m_2 can not be treated independently when computing the system penalty. With $\beta_2 = 0$, we find all the combinations of m_1 and m_2 which generate a fixed distortion-induced-penalty of 0.3 dB. These contributions define the limits of the allowable equivalent transfer function. With $m_1 = m_2 = 0$, the parameter β_2 determines the phase contribution to the distortion-penalties of the equivalent transfer function. The phase contribution to the distortion penalty has a unique value that produces the 0.3 dB distortion penalty. (The 0.3 dB criteria is somewhat arbitrary, but a discussion of why this criteria was chosen is given in detail elsewhere [3]).

6.4 Simulation Results

The simulation consists of finding a contour (Fig. 6.2) representing the contribution of the magnitude to the 0.3 dB distortion-induced eye-closure penalty. Inside the contour, the magnitude contribution is less than 0.3 dB

distortion-penalty; outside the contour, the penalty is higher than 0.3 dB distortion-penalty. Fig.6.3 shows the distortion-induced eye-closure penalty versus the normalized dispersion-like coefficient (β_2). The value of $\beta_2 = 0.65$ radians produces 0.3 dB distortion-induced penalty.

6.5 Example

To illustrate the generality of the above model, we consider a multiwavelength optical network with 30 perfectly aligned (de)multiplexers with 125 GHz bandwidth modeled as third order Butterworth filters. The optical network is considered to be operating first at 10 Gb/s and second at 2.5 Gb/s. The effective magnitude transfer function for the 30 (de)multiplexers is given by:

$$|H(f)| = \left[\frac{1}{1 + \{2(f - f_c) / f_b\}^6} \right]^{30}, \quad (6.10)$$

where f is the optical frequency, f_c is the center frequency of the optical filter, and f_b is the filter 3-dB bandwidth. Table 1 shows the coefficients m_1 and m_2 of the expansion of equation (6.10) for several laser offsets. To evaluate the laser misalignment tolerances at two different bit rate, the coefficients are listed for $B_1 = 2.5$ Gb/s and $B_2 = 10$ Gb/s. The locus of points (m_1, m_2) are plotted as shown in Fig. 6.2 for each bit rate. The crossing of the (m_1, m_2) locus with the 0.3 dB penalty contour gives the laser misalignment tolerances at 0.3 dB distortion-

penalty. This is found to be equal to 41 GHz at 10 Gb/s, and 48 GHz at 2.5 Gb/s. These results are very close to the cases where exact simulations are considered as in reference [4]. Similar techniques can be used for the phase characteristic, and for any other combination of (de)multiplexers.

6.6 Summary

A general (de)multiplexer model is formulated that applies to any bit rate, any filter shape, any filter phase, and any filter bandwidth. The cascade of (de)multiplexers can be represented by an equivalent filter with magnitude equal to the product of all the magnitudes of the multiplexers in the cascade, and phase equal to the sum of all the phases in the cascade. Only one phase term (second order) and two magnitude terms (first and second order) are needed to approximate the system performance of practical cascades.

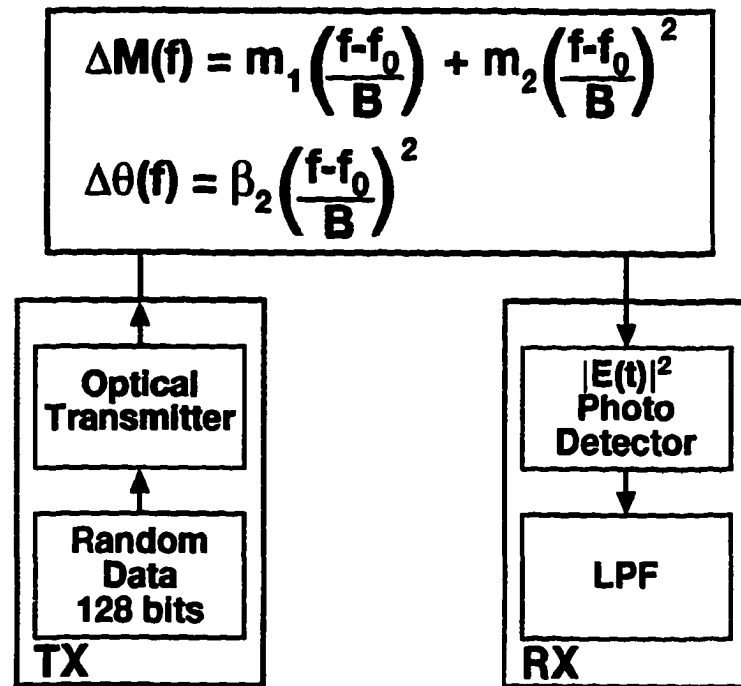


Figure 6.1: Simulation block diagram for a lightwave system where the effective transfer function of the (de)multiplexer cascade is represented by an equivalent filter.

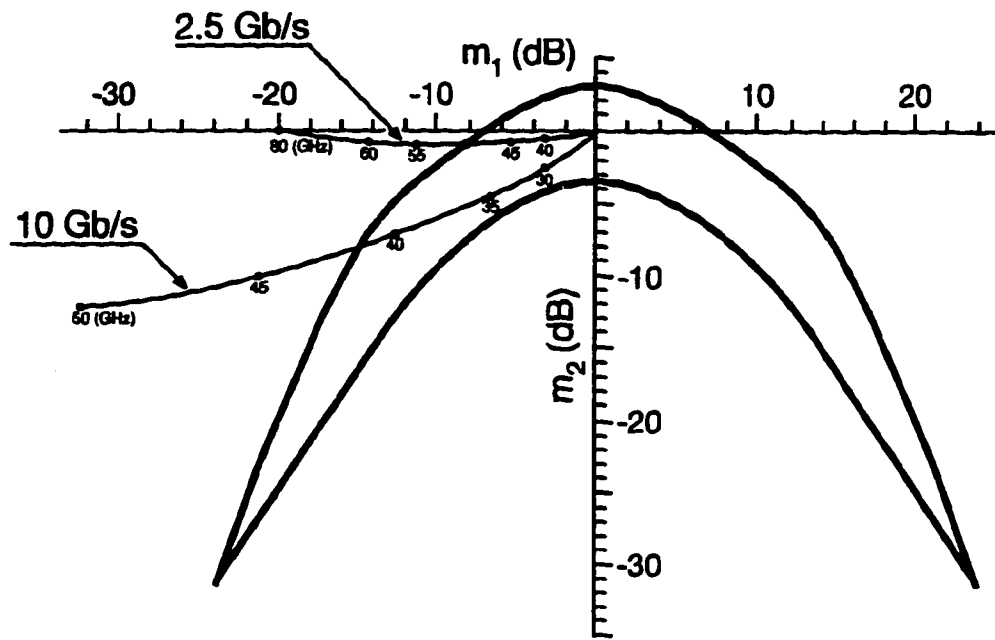


Figure 6.2: A contour at 0.3 dB distortion-induced penalty for all possible combinations of the normalized magnitude coefficients m_1 (X-axis), and m_2 (Y-axis). The Figure illustrates an example for a cascade of 30 (de)multiplexers modeled as 3rd-order Butterworth filters with operation at 10 Gb/s and at 2.5 Gb/s per optical channel. The intersections of the contour and the normalized coefficients for the two bit rates give the allowable laser misalignment tolerances.

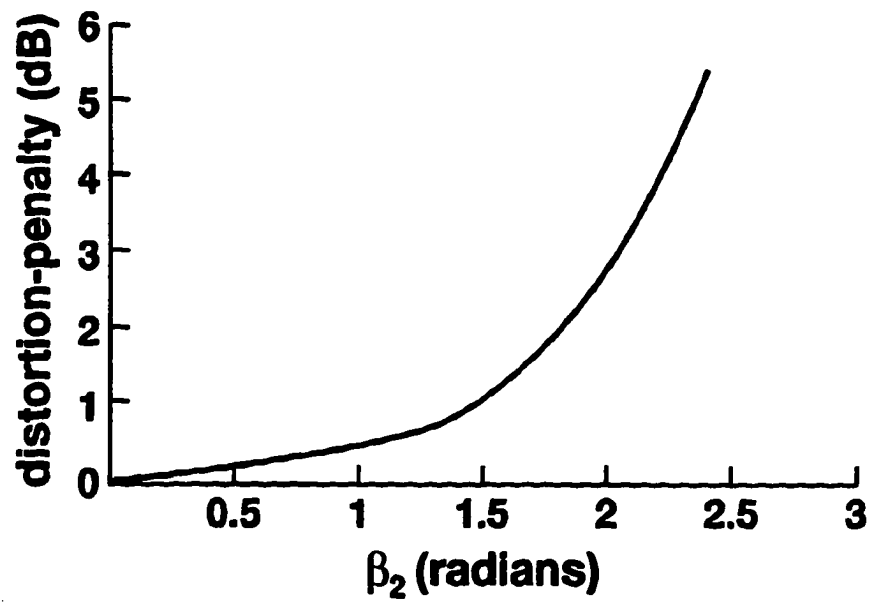


Figure 6.3: Distortion-induced eye-closure penalty versus normalized dispersion-like coefficient β_2 .

f_0 (GHz)	B = 2.5 Gb/s		B = 10 Gb/s	
	m_1	m_2	m_1	m_2
30	-0.79	-0.16	-3.15	-2.58
35	-1.67	-0.29	-6.68	-4.6
40	-3.14	-0.45	-12.57	-7.25
45	-5.30	-0.63	-21.24	-10.07
50	-8.12	-0.76	-32.47	-12.19
55	-11.27	-0.79	-45.07	-12.70
60	-14.30	-0.70	-57.21	-11.28
70	-18.53	-0.34	-74.12	-5.39
80	-19.90	-0.035	-79.61	-0.56

Table 6.1: Magnitude coefficients for 30 filters with $\theta(f) = 0$.

References

- [1] K. C. Kao and G. A. Hockham, "Dielectric fibre surface waveguides for optical frequencies", IEE Proceedings, pp. 1151-1158, 1966.
- [2] F.P. Kapron, D.B. Keck, and R. D. Maurer, "Radiation losses in glass optical waveguides", Applied Physics Letters, vol. 17, pp. 423-425, 1970.
- [3] I. Hayashi, M. B. Panish, P. W. Foy, and S. Sumski, "Junction lasers which operate continuously at room temperature", Applied Physics Letters, vol. 17, pp. 109-111, 1970.
- [4] S. E. Miller and I. P. Kaminow, eds., "Optical Fiber Telecommunications-II", Academic Press, chap. 21, pp. 114-121, 1992.
- [5] W. van Etten and J. van der Plaats, "Fundamentals of optical fiber communications", Prentice Hall, chap. 16, 351-368, 1991.
- [6] A. F. Elrefaie, "Multiwavelength survivable ring network architectures", ICC'93, paper 48.7, Geneva, May 23-26, 1993.
- [7] G. R. Hill, P. J. Chidgey, F. Kaufhold, T. Lynch, O. Sahlen, M. Gustavsson, M. Janson, B. Lagerstrom, G. Grasso, F. Meli, S. Johansson, J. Ingers, L. Fernandez, S. Rotolo, A. Antonielli, S. Tebaldini, E. Vezzoni, R. Caddedu, N. Caponio, F. Testa, A. Scavennec, M. J. O'Mahony, J. Zhou, A. Yu, W. Sohler, U. Rust, and H. Hermann., "A transport network layer based on optical network elements", J. Lightwave Technol. vol. 11, pp. 667-679, 1993.

- [8] K. T. Koai, "Integrating video and information transport into survivable interoffice networks", ICC'94, Paper 331.4, New Orleans, May 1-3 , 1994.
- [9] W. J. Tomlinson and R. E. Wagner, "Wavelength division multiplexing-Should you let it in your network?", NFOEC'93, Paper 19.4, San Antonio, June 13-17, 1993.
- [10] K. I. Sato, S. Okamoto, and H. Hadama, "Network performance integrity enhancement with optical path layer technologies", IEEE J. Selected Areas in Common. vol. 12, pp.159-170, 1994.
- [11] K. Hirabayashi and T. Kurokawa, "Tunable wavelength-selective demultiplexer using a liquid-crystal filter", IEEE Photon. Technol. Lett., vol. 4, pp. 737-740, 1992.
- [12] G. K. Chang, M. Z. Iqbal, K. Bala, G. Ellinas, J. Young, H. Shirokman, C.E. Zah, L. Cutus, B. Pathak, D. Mahoney, J. Gamelin, E. Goldstein, L. Eskildsen, and C. A. Brackett, "Experimental demonstration of a reconfigurable WDM/ATM/SONET multiwavelength network testbed", OFC'94 paper PD9, Feb. 1994.
- [13] C. Dragone, C. A. Edwards, and R. C. Kistler, "Integrated optics NXN multiplexer on silicon", IEEE Photon. Technol. Lett., vol. 3, pp. 896-899, 1991.

- [14] H. Takahashi, et al., "Polarization-Insensitive arrayed-waveguide wavelength multiplexer with birefringence compensating film", *IEEE Photon. Technol. Lett.*, vol. 5, pp. 707-709, 1993.
- [15] M. R. Amersfoort, et al., "Low-loss phased-array based 4-channel wavelength demultiplexer integrated with photodetectors", *IEEE Photon. Technol. Lett.*, 6, 62-64, 1994.
- [16] Charles A. Brackett, et al., "A scalable multiwavelength multihop optical network: a proposal for research on all-optical networks", *J. Lightwave Technol.* vol. 11., pp.736-753, May/June, 1993.
- [17] A. R. Chraplyvy, "Limitations on lightwave communications imposed by optical fiber nonlinearities", *J. Lightwave Technol.* vol. 8, pp. 1548-1557, 1990.
- [18] P. J. Smith, D. W. Faulkner and G. R. Hill, "Evolution scenarios for optical telecommunication networks using multiwavelength transmission" *Proc. IEEE*, 81, pp. 1580-1587, 1993.
- [19] C. S. Li, F. F. K. Tong, K. Liu, and D. G. Messerschmitt, "Channel capacity optimization of chirp-limited dense WDM/WDMA systems using OOK/FSK modulation and optical filters", *J. Lightwave Technol.*, vol 10, pp.1148-1161, 1992.
- [20] N. N. Khrais, A. F. Elrefaie, and R. E. Wagner, "Performance degradations due to laser and optical filter misalignments in WDM systems", *OFC'95*, Paper TuC5, Feb. 1995.

- [21] D. R. Wisely, "32 channel WDM multiplexer with 1-nm channel spacing and 0.7 nm bandwidth", *Electron. Lett.* vol. 27, pp. 520-521, 1991.
- [22] K. Uomi, A. Murata, S. Sano, R. Takeyara, and A. Takai, "Advantage of 1.55 μ m InGaAs/InGasp MQW-DFB lasers for reducing waveform degradation and dispersion penalty for 2.5 Gbps lon-span normal fiber transmission", *IEEE Photon. Technol. Lett.*, vol. 4, pp. 657-660, 1992.
- [23] N. N. Khrais, , A. F. Elrefaie, and R. E. Wagner, "Performance degradation of WDM systems due to laser and optical filter misalignments" *IEE Electron. Lett.*, vol. 31 pp. 1179-1180, 1995.
- [24] C. E. Zah, F. J Favire, B. Pathak, R. Bhat, C. Caneau, P. S. D Lin, and A. S. Gozdz, "Monolithic integration of multiwavelength compressive-strained multi-quantum-well distributed-feedback laser array with star coupler and optical amplifiers", *IEE Electron. Lett.*, vol. 28, pp. 2361-2362, 1992.
- [25]] N. N. Khrais, , A. F. Elrefaie, R. E. Wagner, and Samir Ahmed, "Performance degradation of multiwavelength optical networks due to laser and (de)multiplexer misalignments", *IEEE Photon. Technol. Lett.*, vol. 7, pp. 1348-1350, 1995.
- [26]] N. N. Khrais, , A. F. Elrefaie, R. E. Wagner, and Samir Ahmed, " Effect of cascaded misaligned optical (de)multiplexer on multiwavelength optical network performance, OFC'96, Paper ThD4, San Jose, Feb. 25-March 1, 1996.

- [27] Adel A. M. Saleh, "Overview of the MONET, multiwavelength optical networking, program", OFC'96, paper ThI3, San Jose, Feb. 25-March 1, 1996.
- [28] R. E. Wagner, R. C. Alferness, A. A. Saleh, M. C. Goodman, "MONET: multiwavelength optical networking", J. Lightwave Technol. vol. 11, pp. 1349-1355, 1996.
- [29] N. N. Khrais, F. Shehadeh, J.-C. Chiao, R. S. Vodhanel, and R. E. Wagner, "Multiplexer eye-closure penalties for 10 Gb/s signals in WDM networks, OFC'96, paper PD33, San Jose, Feb. 25-March 1, 1996.
- [30] N. N. Khrais, , A. F. Elrefaie, R. E. Wagner, and Samir Ahmed, "Performance of cascaded misaligned optical (de)multiplexers in multiwavelength optical networks", IEEE Photon. Technol. Lett., vol.8, pp. 1073-1075, 1995.